이학박사학위논문

Studies on mitochondrial targeting and protein sorting mechanisms via transmembrane domains of inner membrane proteins in yeast mitochondria

미토콘드리아 막 단백질의 표적화와 막 내 삽입 기작에 관한 연구

2023 년 2 월

서울대학교 대학원

생명과학부

이 서 은

Studies on mitochondrial targeting and protein sorting mechanisms via transmembrane domains of inner membrane proteins in yeast mitochondria

by

Seoeun Lee

Under the supervision of

Professor. Hyun Ah Kim, Ph.D.

A thesis submitted in partial fulfillment

of the requirements for the degree of

Doctor of Philosophy

February 2023

School of Biological Science

Seoul National University

미토콘드리아 막 단백질의 표적화와 막 내 삽입 기작에 관한 연구

Studies on mitochondrial targeting and protein sorting mechanisms via transmembrane domains of inner membrane proteins in yeast mitochondria

지도교수 Hyun Ah Kim

이 논문을 이학박사 학위논문으로 제출함
2023 년 02 월

서울대학교 대학원
생명과학부
이 서 은

이서은의 이학박사 학위논문을 인준함
2023 년 2 월

위 원 장 _____ 석 영 재 (인)

부위원장 _____ Hyun Ah Kim (인)

위 원 _____ 허 원 기 (인)

위 원 _____ 조 형 택 (인)

위 원 _____ Hun sang Lee (인)

ABSTRACT

Studies on Mitochondrial Targeting and Protein Sorting mechanisms via Transmembrane domains of inner membrane proteins in yeast mitochondria

Seoeun Lee

School of Biological Science

Seoul National University

Most mitochondrial proteins are encoded in the nuclear genome and these proteins play vital roles in biogenesis of the respiratory chain complex, maintaining mitochondrial protein homeostasis and dynamic fission and fusion of mitochondria and so on. A failure in the biogenesis of these nuclear-encoded mitochondrial proteins is detrimental to the organism. Thus, elucidating how these proteins are generated is essential not only for understanding the principle of life but also for developing therapeutics of mitochondrial-related diseases.

During the synthesis of the nuclear-encoded mitochondrial proteins in cytosol, they must be correctly targeted to mitochondria and transported into the sub-organelle compartments. For the targeting to mitochondria, these proteins possess the N-terminal mitochondrial targeting sequence (MTS). After targeting to the outer membrane of mitochondria (OM), proteins are translocated across the OM through the translocase of the outer membrane (TOM) complex. Among those proteins, proteins which are supposed to be located in mitochondria matrix or inner membrane of mitochondria (IM) are sorted via the translocase of the inner membrane (TIM) complex in the IM. It has been known that unfolded or unassembled IM proteins can be degraded by the IM-resident protease, *m*-AAA complex in the inner membrane to maintain homeostasis of mitochondria. This study aims to detailed understand 1) molecular mechanism of *m*-AAA protease complex for membrane protein sorting, 2) effects of Mgr2, a subunit of the TIM complex on membrane protein efficiency into the IM and 3) Mitochondrial protein targeting in *Saccharomyces cerevisiae.*

For these purposes, the study aimed to elucidate molecular functions of membrane-anchor domain of *m*-AAA domain in *m*-AAA-dependent IM-protein dislocation into the matrix. For this, dislocation of model Mgm1 variants was assessed in Yta10 and

Yta12 mutants where TM domains of them were replaced with ones of unrelated proteins (Chapter 1). Here, I found that the second TM domain of Yta10/12 is critical for dislocation of the IM-proteins.

Next, to analyze effects of Mgr2, a gatekeeper of the TIM complex on the membrane insertion efficiency depending on characteristics of its precursors, a known TIM complex-substrate Mgm1 variants in the hydrophobicity of the presence of flanking charged amino acids in the membrane-sorting signal were tested in mgr2 deletion and mgr2 overexpression strains (Chapter 2). Here, this study found that precursors with moderately hydrophobic membrane-sorting signal and positively charged amino acids flanking the membrane-sorting signal are critical for Mgr2-dependent membrane sorting regulation.

Lastly, this study I aimed first to investigate what factors of MTS are critical for efficient protein targeting to mitochondria. For this, the targeting efficiency of a set of MTS versions varying the length, hydrophobicity and charged amino acids of MTS were tested by yeast growth complementation assay, subcellular fractionation and fluorescence microscopy (Chapter 3). Here, this study found that the certain length of MTS and position of charged amino acids are critical for protein targeting efficiency.

Taken together, these results demonstrate the missing puzzles on the molecular principles of MTS-mediated mitochondrial proteins targeting to mitochondria and Mgr2 and *m*-AAA protease dependent protein sorting in the IM.

Keyword: Mitochondrial targeting sequence, Mgr2, *m*-AAA protease, Mitochondria, Yeast

Student Number: 2015-30981

CONTENTS

LIST OF FIGURES

CHAPTER 3. Yta10 targeting factors are elucidated for the mitochondrial targeting *in vivo*

LIST OF ABBREVIATIONS

MTS	Mitochondrial targeting sequence
OM	Outer membrane
TOM	Translocase of outer membrane
IM	Inner membrane
TIM	Translocase of inner membrane
IMS	Intermembrane space
AAA	ATPases Associated with diverse cellular Activities
MPP	Matrix processing peptidase
TM	Transmembrane
PAM	Presequence translocase associated Motor
PBE	Puf3 Binding Element
yEGFP	yeast Enhanced Green Fluorescent Protein

CHAPTER 1

m-AAA protease–mediated dislocation of TM domains in the mitochondrial IM

1.1. Introduction

Most mitochondrial proteins are encoded from the nuclear genome, translated and delivered to the mitochondria. About the two third of the mitochondrial proteins contain the N-terminal mitochondria targeting sequence (MTS) which is also called presequence. The MTS mediates targeting of precursors to mitochondria, encountering the translocase of outer membrane (OM), TOM complex, which is the first entry site of all mitochondrial proteins (Figure 1). More detail of the TOM complex will be discussed later in the chapter III.

The mitochondrial inner membrane(IM)

About 40% of the total mitochondrial proteome resides in the inner membrane (IM), making the IM the most protein-rich membranes in mitochondria [1]. In addition, since the IM proteome consists of both nuclear and mitochondrial genome-encoded membrane proteins, expression level, sorting and assembly of those IM-proteins have to be precisely coordinated. Failure in these processes in the IM can easily compromise protein homeostasis in the IM, potentially causing proteotoxicity. Therefore, the IM require surveillance system to search and get rid of misfolded and misassembled proteins. It has been shown that two ATP-dependent proteases, the *i*-AAA (intermembrane space) and *m*-AAA (catalytic site facing matrix) proteases that belong to the FtsH (Filamentous temperature sensitive H) peptidase family play a central role in protein degradation in the IM [2-4].

The TIM23 complex

The TIM23 complex is a translocase in the IM and mediates the import of precursor proteins that have N-terminal presequence into the matrix and the integration of hydrophobic segments into the IM.

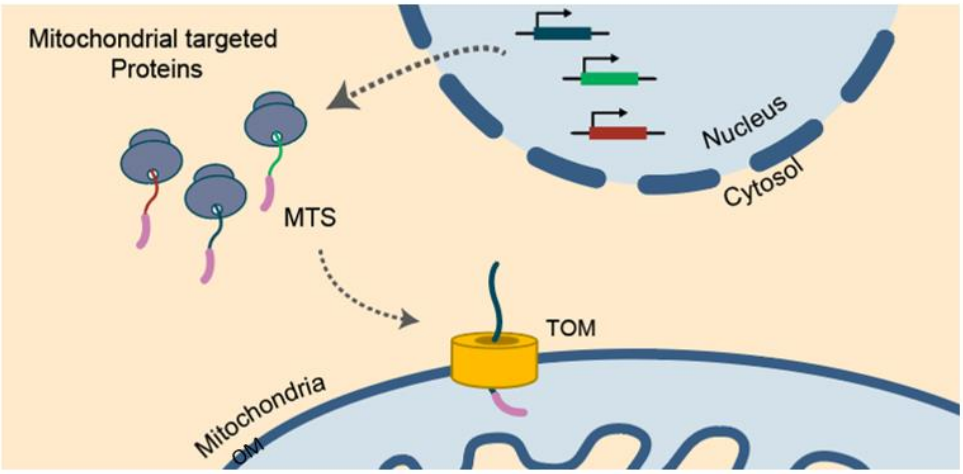

Figure 1. Proteins targeting to mitochondria are first directed to the TOM complex in the outer membrane (OM). Most mitochondrial proteins are translated in the cytosol and then delivered to the mitochondria. ~2/3 of mitochondrial proteins contain N-terminal cleavable mitochondria targeting sequence (MTS). After MTS-mediated targeting to mitochondria, these proteins enter mitochondria via the TOM complex, which is the first entry site of mitochondrial proteins

The m-AAA protease

The *m*-AAA protease form a major quality control system in the mitochondrial IM and mediate the degradation of misfolded or unassembled mitochondrial IM proteins [5-9]. The *m*-AAA protease is one of the AAA-ATPases (ATPase Associated with diverse cellular Activities) and anchored in the IM with its large soluble catalytic domain facing the matrix. This protein complex is conserved from prokaryote (FtsH), yeast (Yta10 and Yta12), to human (AFG3L2 and SPG7) [5, 10]. The *m*-AAA protease is a hetero-hexameric complex composed of Yta10 and Yta12; each contains two N-terminal TMs, a soluble AAA+ domain, and a proteolytic domain exposed to the matrix (Figure 2) [3, 11].

In addition to quality control, *m*-AAA protease helps protein folding of a mitochondrial ribosome subunit, MrpL32 [12], and maturation of cytochrome c peroxidase (Ccp1) [13] . The complex acts on not only protein processing and maturation of a subset of proteins [14] .

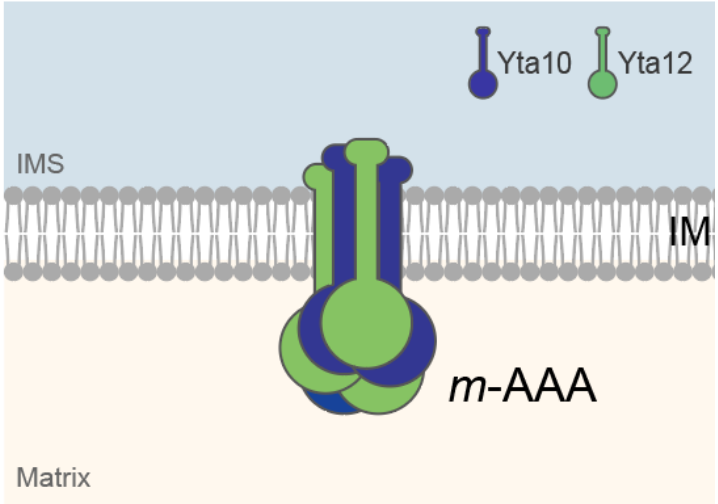

Figure 2. *m*-AAA protease is composed of Yta10 and Yta12 at the IM. The *m*-AAA protease forming a hetero-hexameric complex composed of Yta10 and Yta12. Each subunit has membrane anchored domain and large soluble catalytic domain facing matrix side.

Dislocation Activity

It has been suggested that the protein dislocation activity is conserved throughout the AAA proteases [9, 10]. Misfolded or non-assembled membrane proteins are extracted from the membrane for proteolysis by the AAA proteases [15, 16]. Protein segments that are protruded from the membrane surface are sufficient to allow *m*-AAA protease-dependent degradation in the matrix side [16].

For the maturation of the Cytochrome c peroxidase (Ccp1) which resides in IMS, the *m*-AAA protease and the rhomboid protease Pcp1 are required [13]. The *m*-AAA protease mediates the ATP-consuming dislocation of Ccp1 from the membrane to the matrix, independent of its proteolytic activity. The dislocation requires positioning of the hydrophobic segment of Ccp1 in the IM for intramembrane cleavage by the rhomboid protease, Pcp1 in the IM (Figure 3). Mammalian *m*-AAA proteases can substitute for the yeast homologue in protein processing [17, 18] implying that the ability for protein dislocation of the *m*-AAA complex is conserved.

One of the roles of the *m*-AAA complex is to process the mitochondrial ribosomal subunit, MrpL32 which regulates ribosome biogenesis and the formation of respiratory complexes [3, 12, 13, 17, 19]. Mutations in the catalytic domains of the *m*-AAA protease impair MrpL32 processing, thereby yeast growth in respiratory conditions. Oxidative stress leads to misfolding of MrpL32, resulting in its degradation by the *m*-AAA protease and decreased mitochondrial translation [12, 13].

In the case of Ccp1 maturation, the *m*-AAA protease acts as an ATPase by pulling the Ccp1 TM to the matrix prior to processing by a rhomboid protease, Pcp1, in the IM [20]. Furthermore, an earlier study has shown that moderately hydrophobic TM domains can be dislocated by the *m*-AAA protease [21].

This study investigated the molecular mechanism of the m-AAA protease–mediated TM helix dislocation, and focused on the role of TM domain of the *m*-AAA protease in *Saccharomyces cerevisiae.*

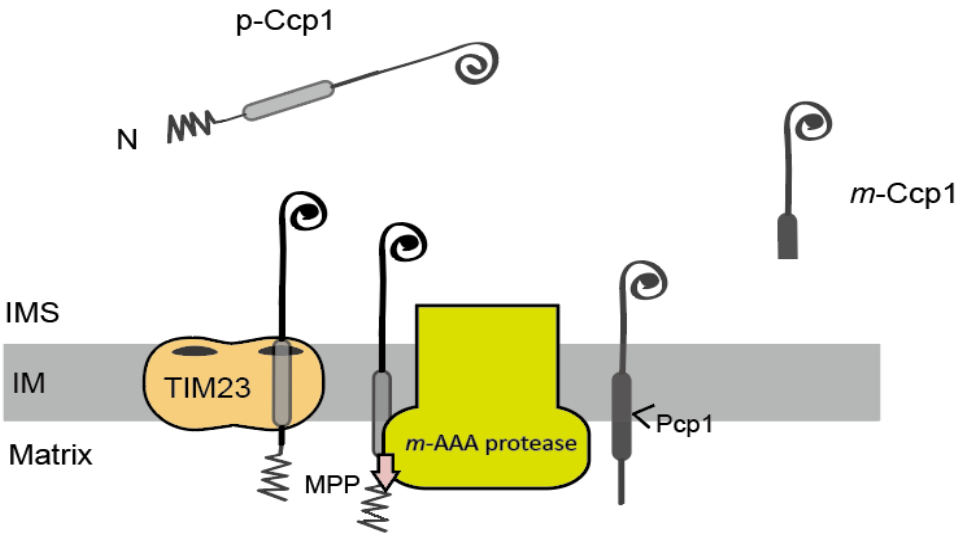

Figure 3. Ccp1 maturation is mediated by dislocation activity of the *m*-AAA protease. Premature Ccp1 (*p*-Ccp1) goes to the TIM23 complex, then is dislocated by the *m*-AAA protease. Dislocated Ccp1 at the TM1 is recognized and cleaved by the Pcp1, and matured to the *m*-Ccp1. MTS of Ccp1 is cleaved by the matrix processing peptidase (MPP).

1. 2. Results

1. 2. 1. Yta10 or Yta12 variants with a replaced TM domain complement respiratory growth defect

To investigate the role of the TM domains of the *m*-AAA protease on the membrane insertion and dislocation of substrate proteins, respective TM domains of Yta10 and Yta12 were replaced by TM domains of a IM protein Mdl2, which is known to be non-associated with protein insertion and processing processes in the IM (RTM1 or RTM2 for Yta10 and Yta12) (Figure 4) [22]. Then, to see whether the RTM1 and RTM2 versions are properly localized to the IM and functional, yeast growth complementation assay was performed (Figure 5). The *yta10*Δ and *yta12*Δ strains were viable on fermentable condition, but not on respiratory condition as previously shown [12]. The RTM1/2 versions of Yta10 or Yta12 were expressed in the *yta10*Δ and *yta12*Δ strains and the growth of these strains were restored in respiratory growth condition.

1. 2. 2 Yta10 and Yta12 RTM variants have no defects in processing of MrpL32

To check whether the protein processing activity of RTM1/2 versions of Yta10/12 works efficiently, protein processing of a well-known *m*-AAA protease substrate, MrpL32 was tested in the Yta10/12 RTM1/2 strains. Reduced processing of MrpL32 in the *yta10*Δ and *yta12*Δ strains were restored to the level of that in the WT strain (Figure 5).

These results suggest that the Yta10 or Yta12 variants with a replaced TM domain are correctly targeted to the IM, assembled into the *m*-AAA protease complex, and have normal protein processing activity.

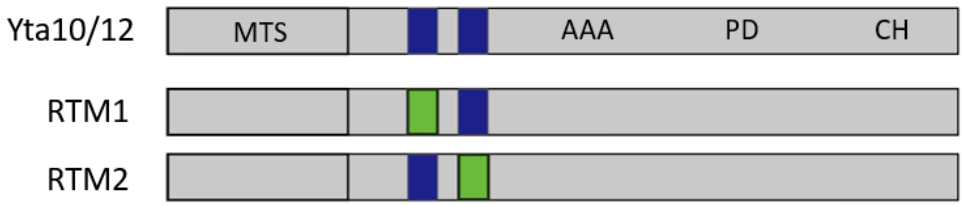

Figure 4. Yta10 and Yta12 variants with a replaced TM. A, schematics of Yta10 and Yta12 with TMs highlighted in blue. AAA, AAA domain; PD, proteolytic domain; CH, C-terminal helical domain. TM domains of Yta10 and Yta12 were replaced by TM domains of a IM protein Mdl2, one at a time.

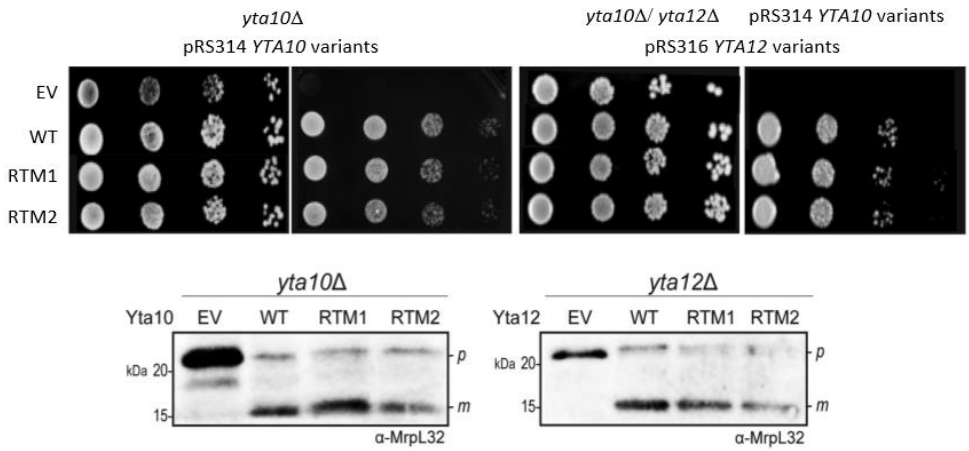

Figure 5. Yta10 and Yta12 variants with a replaced TM are functional. Yta10 or Yta12 variants were expressed in *yta10*Δ (*upper, left panel*) or *yta10*Δ/ *yta12*Δ [pRS314 YTA10 WT] (*upper, right panel*), respectively, under the endogenous promoter. The transformants were cultured in glucose-containing liquid medium prior to spotting on YPD (fermentation condition) or YPEG (respiration condition) plates. The plates were incubated at 30 °C for 2 days prior to imaging. EV, empty vector; RTM1, replaced TM1; RTM2, replaced TM2. (*lower panel*) Maturation of MrpL32. *yta10*Δ or *yta10*Δ/ *yta12*Δ [pRS314 YTA10 WT] cells expressing Yta10 or Yta12 variants were cultured overnight and lysed in sample buffer. The lysates were analyzed by SDS-PAGE and Western blotting. The blots were immunoblotted with α-MrpL32 antibody. *p*, precursor; *m*, mature form

1. 2. 3. Substrates to assess dislocation activity of the Yta10 and Yta12 RTM variants Mgm1(nL/ (19-n)A) variants, and model proteins

Mgm1 is known to play a role in fusion of mitochondria and naturally exists in two isoforms; long(*l*)-Mgm1 and short(*s*)-Mgm1. It carries an N-terminally located mitochondrial targeting sequence (MTS) followed by two putative TM domains. The insertion efficiency of the Mgm1 TM1 segment into the IM is roughly 50%, generating the *l*-Mgm1. For those Mgm1 TM1 that are not membrane inserted is translocated into the matrix and the TM2 segment subsequently enters into the IM where it is further processed by Pcp1, a protease in the IM, producing the *s*-Mgm1 (Figure 6, *left*). The sorting of the TM1 segment of Mgm1 between the IM and the matrix occurs at the level of the TIM23 complex, not by the *m*-AAA protease.

However, when the TM1 of Mgm1 is replaced with a non-natural TM domain, a set of 19 amino acid stretches composed of n leucines and (19-n) alanines, most of Mgm1 variants are laterally released into the IM and then, they can be further dislocated into the matrix by the *m*-AAA protease, exposing TM2 to the IM-resident Pcp1 to produce the *s*-Mgm1 (Figure 7, *right*). This dislocation efficiency by the *m*-AAA complex is shown to be dependent on the hydrophobicity of the TM1; moderately hydrophobic TM1 tends to be more dislocated than highly hydrophobic ones. Thus, for the Mgm1 carrying the engineered TM1 domain (nL/ (19-n)A) constructs), the generation of *s*-Mgm1 is thus dependent on the dislocation activity of the *m*-AAA protease.

To distinguish whether the *m*-AAA protease TM2 causes a general defect in membrane dislocation activity or in recognizing their substrates, previously characterized *m*-AAA protease substrates were introduced. Ccp1 is a natural substrate of the *m*-AAA protease. For Ccp1 biogenesis, precursor Ccp1 is dislocated by the *m*-AAA protease to position for cleavage in the matrix and Pcp1 in the IM (Figure 8, *left*).

Another example, Cox5aT-MFP (MFP, Mgm1 fusion protein) is a chimera protein, where Cox5a protein is truncated at residue 128 and fused to the C terminus of Mgm1 [23]. Previous studies have shown that this C-terminal truncation at the IMS side converts Cox5a into the *m*-AAA protease substrate (Figure 8, *right*).

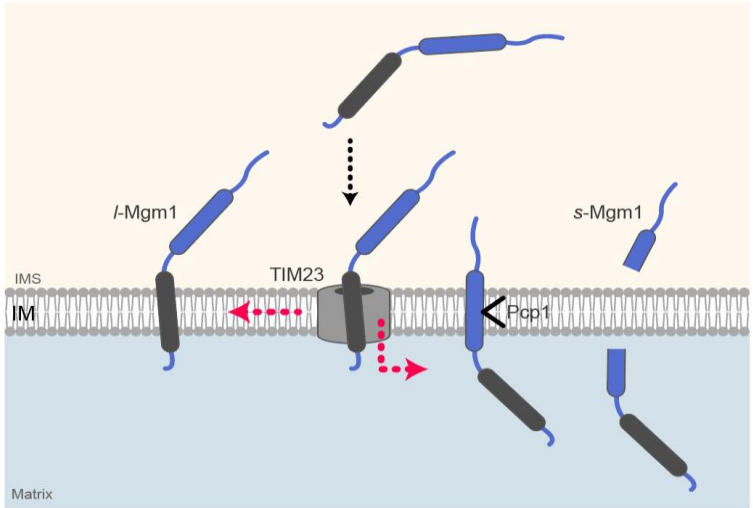

Figure 6. Mgm1 is sorted by the TIM23 complex called alternative topogenesis. Mgm1 TM1 and TM2 are hydrophobic and indicated by dark gray boxes, respectively. The TIM23 complex recognizes *p*-Mgm1, sorts Mgm1, then generates *l*-Mgm1 and *s*-Mgm1. Processing by Pcp1 only occurs when the cleavage site in the TM2 reaches the inner membrane. IMS, intermembrane space; IM, inner membrane; MPP, mitochondrial processing peptidase; *p*-Mgm1, precursor protein of Mgm1; *l*-Mgm1 and *s*-Mgm1, large and short isoform of Mgm1, respectively.

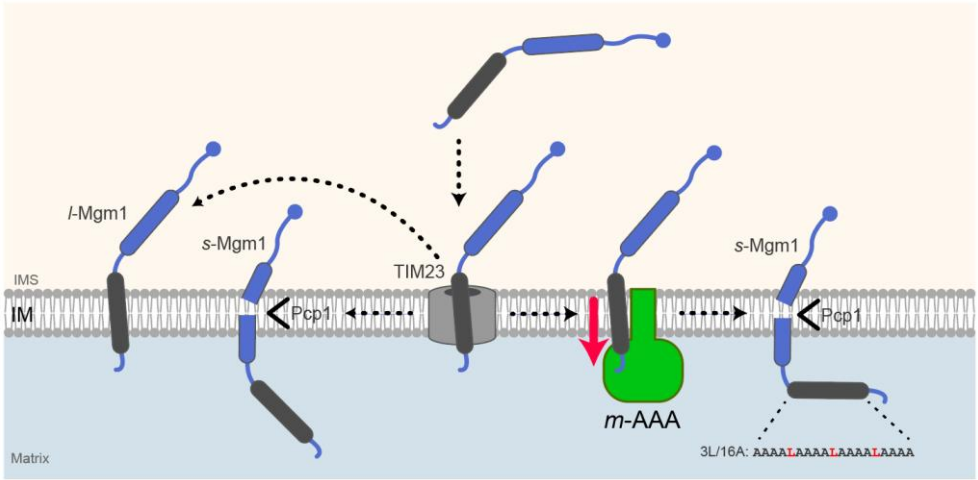

Figure 7. Mgm1(nL/ (19-n)A) is dislocated by the *m*-AAA protease. Mgm1(nL/ (19-n)A) passes TIM23 complex, first, and TM1 is dislocated from the IM. Some is generation of *l*-Mgm1, and the rest id made *s*-Mgm1, result of Pcp1.

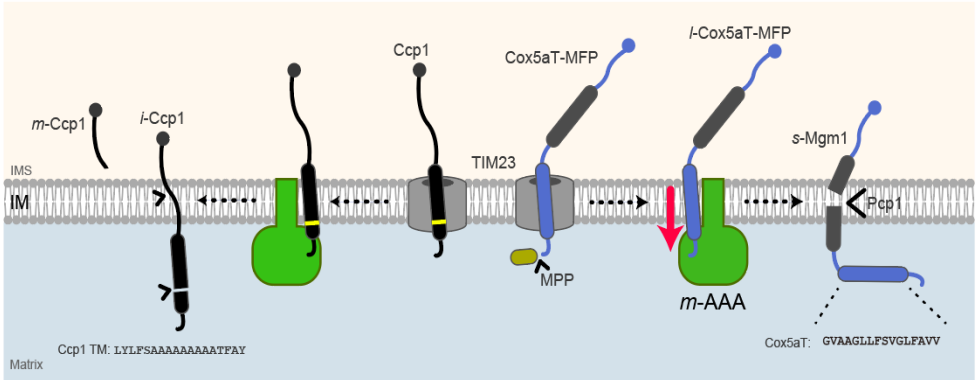

Figure 8. Ccp1 and Cox5aT- MFP are dislocated by the *m*-AAA protease. Ccp1 and Cox5aT- MFP passes TIM23 complex, and TM1(or putative TM) is dislocated from the IM. Some is generation of *l*-Mgm1, and the rest is made *s*-Mgm1, result of Pcp1.

2. 3. Replacement of the TM2 domain of Yta10 and Yta12 impairs membrane dislocation of model Mgm1 protein

To assess the effects of TM1/ 2 of Yta10/12 on the dislocation activity of the *m*-AAA protease, a set of Mgm1(nL/ (19-n) A) constructs was expressed in the *yta10*Δ or *yta12*Δ strain carrying each Yta10 and Yta12 RTM variant. If the role of Yta10 or Yta12 TM domains is limited to anchor the *m*-AAA protease in the membrane with catalytic domain (ATPase domain and the metalloprotease domain) facing the matrix, the substitution of TM domains would have minimal effect on its dislocation activity. However, if the TM domains of Yta10 or Yta12 are required either for substrate recognition or protein dislocation, the substitution of Yta10/ Yta12 TM domains would compromise the protein dislocation activity of the *m*-AAA protease.

The ratio of *l*-Mgm1 to *s*-Mgm1 in the *yta10*Δ or *yta12*Δ strain carrying Yta10/12 RTM1 mutants was comparable to those carrying Yta10 or Yta12 WT (Figure 9), although a subtle decrease in the dislocation of 5L/14A TM domain (Mgm1(5L/ 14A)) was observed in both Yta10 and Yta12 RTM1s (Figure 9). In comparison, the replacement of the TM2 (RTM2) of Yta10/12 significantly reduced generation of *s*-Mgm1, indicating that the membrane dislocation activity is severely impaired upon replacement of the TM2 domain of the *m*-AAA protease subunits (Figure 9).

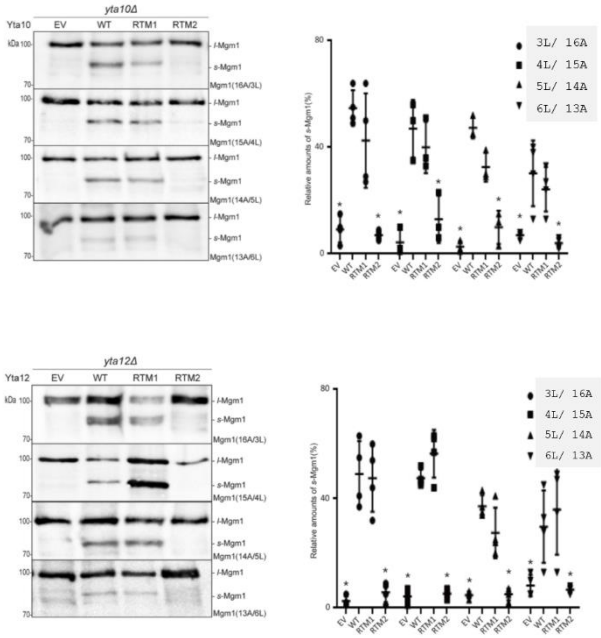

Figure 9. Dislocation of Mgm1(nL/ (19-n)A) requires TM2 of Yta10 and Yta12.

The sequences of the TM1 segment of Mgm1, Mgm1 (3L/ 16A, 4L/ 15A, 5L/ 14A, 6L/ 13A) are shown. A, Dislocation of Mgm1(nL/ (19-n)A). Yeast transformants expressing the indicated Yta10 variant and Mgm1(nL/ (19-n)A) were lysed in the presence of 25% TCA (final concentration). The lysates were analyzed by SDS-PAGE and Western blotting. The blots were immunoblotted with α-HA antibody, which detects the HA tag at the C terminus of Mgm1(nL/ (19-n)A). Relative amounts of *s*-Mgm1 were quantified from three independent experiments and plotted with standard deviations. A *t*-test was performed to examine the statistical significance of the observed results (*upper*). C, Yta12 variants were tested in the same manner as described in *upper* (*lower*) The differences in dislocation efficiency were statistically significant between WT and EV/RTM2 (*, $p < 0.05$).

2. 4. Replacement of the TM2 domain of Yta10 selectively impairs membrane dislocation for only Mgm1 variant

To further dissect the role of TM2s of Yta10/12 in protein dislocation activity or substrate recognition, other *m*-AAA protease substrates with different features were tested.

Ccp1 is a natural substrate of the *m*-AAA protease. For maturation of Ccp1, a precursor form undergoes two-step cleavage first by the *m*-AAA protease in the matrix and second by Pcp1 at the IM. The Ccp1 and replacement of Ccp1 TM1 with 4 leuciens and 15 alanines (Ccp1(4L/15A)) do not affect its normal processing. For the Ccp1, membrane dislocation efficiency is measured by the amount of mature Ccp1 (*m*-Ccp1) (Figure 10).

Another substrate, Cox5aT- MFP (MFP: Mgm1 fusion protein) is a chimera protein that Cox5a protein is truncated at the residue 128 from 153 and fused to the C-terminus of Mgm1. Previous studies have shown that this C-terminal truncation at the IMS side converts Cox5a into the *m*-AAA protease substrate. In addition to CoxtaT-MFP, Cox5aT (4L/ 15A)-MFP was prepared by replacing Cox5a TM domain with a stretch of 4 leuciens and 15 alanines to match the hydrophobicity of that of Mgm1 and Ccp1. Membrane dislocation efficiency of Cox5aT-MFP variants was measured by assessing the formation of *s*-Mgm1 (Figure 10, *upper*).

First, membrane dislocation efficiency of Ccp1, Cox5aT-MFP, and their variants in the cells carrying the Yta10 RTMs was assessed. In contrast to the results with Mgm1 nL/ (19-n) variants, the generation of *m*-Ccp1 or *s*-Mgm1 in Yta10 RTM2 strain was comparable to that of the cells carrying Yta10 WT, indicating that dislocation of Ccp1 and Cox5aT-MFP variants were unaffected by the TM2 replacement of Yta10 (Figure 10, *lower*).

These results thus show that the replacement of Yta10 TM2 domain impairs dislocation of Mgm1 variant but not Ccp1 or Cox5aT-MFP variants, exhibiting a substrate-selective impairment for the membrane dislocation activity of the *m*-AAA protease.

2. 5. Replacement of the TM2 domain of Yta12 causes a general defect in membrane dislocation activity of the m-AAA protease

Next, the dislocation efficiency of Ccp1 and Cox5aT-MFP variants were tested in the cells carrying the Yta12 RTMs. The generation of *m*-Ccp1 or *s*-Mgm1 was significantly reduced compared to the cells carrying Yta12 WT, indicating that the

membrane dislocation of tested substrates was severely impaired (Figure 11).

This suggests that the replacement of the TM2 domain of Yta12 causes a general defect in membrane dislocation activity of the *m*-AAA protease, different from the effects of the TM2 replacement of Yta10.

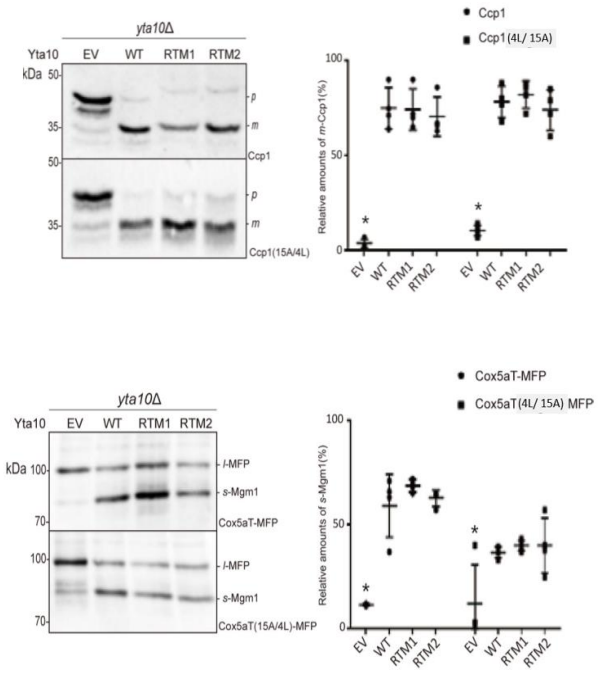

Figure 10. Dislocation activity is unaffected in Yta10 RTM2. Expression of Ccp1, Ccp1(4L/ 15A) (*upper*), Cox5aT-MFP, or Cox5aT (4L/ 15A) –MFP (*lower*) in *yta10*Δ strain carrying the indicated Yta10 variants. Lysates were prepared and analyzed as described in Figure 9. Relative amounts of *m*-Ccp1 or *s*-Mgm1 were quantified with standard deviations. A *t*-test was performed to examine the statistical significance of the observed results. *l*-MFP, long Mgm1 fusion protein.

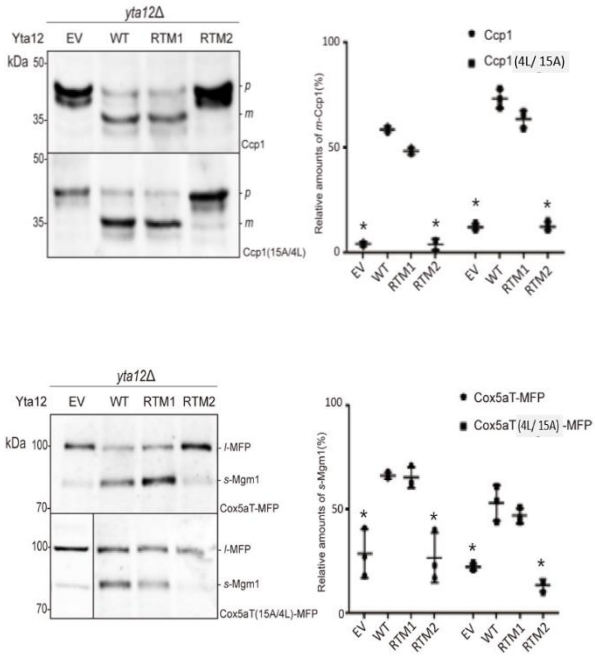

Figure 11. Dislocation activity is defective in Yta12 RTM2. Expression of Ccp1, Ccp1(4L/ 15A) (*upper*), Cox5aT-MFP, or Cox5aT (4L/ 15A) –MFP (*lower*) in *yta12*Δ strain carrying the indicated Yta10 variants. Lysates were prepared and analyzed as described in Figure 9. Relative amounts of *m*-Ccp1 or *s*-Mgm1 were quantified with standard deviations. A *t*-test was performed to examine the statistical significance of the observed results. *l*-MFP, long Mgm1 fusion protein. The differences in dislocation efficiency were statistically significant between WT and EV/RTM2 (*, $p < 0.05$).

2. 6. Dislocation of a TM domain with a hydrophilic IMS moiety is inhibited in the length dependent manner

When the *m*-AAA protease mediates degradation of a membrane protein, not only the TM domains but loop regions in the IMS should be pulled across the IM. To determine the dislocation capacity of the *m*-AAA protease, a hydrophilic segment containing many polar and charged residues from the *Escherichia coli* leader peptidase periplasmic (P2) domain was introduced in between the two TM domains of Mgm1(4L/ 15A) at various lengths; 24, 50, and 105 a.a long (Figure 12).

Dislocation of the TM1 segment of Mgm1(4L/ 15A) was gradually decreased by 24 and 50 amino acid long extensions and completely inhibited by 105 amino acid long extensions (Figure 12). Earlier study has shown that a tightly folded domain in the downstream of the TM domain prevents membrane protein degradation by the *m*-AAA protease [12]. To check whether the hydrophilic segments used in our experiment form a tightly folded structure, the structure of the P2 domain was examined from the protein data bank (PDB 1T7D) [24]. 24 and 50 amino acid long segments are mostly unstructured and a 105 amino acid segment consists of some β-strands and unstructured loops. Thus, it is unlikely that membrane dislocation was prevented due to the folding structure of the hydrophilic extension. These results thus suggest that the *m*-AAA protease has limited capacity to dislocate a large IMS moiety.

If dislocation occurs through hydrophobic core of the lipid membrane, large energy is required, therefore long hydrophilic extension would prevent membrane dislocation whereas if it occurs through a proteinaceous pore, the energy barrier would be lower and the extension length would less influence dislocation efficiency. To test the translocation efficiency of P2 domain through the proteinaceous channel, increasing length of hydrophilic extensions added in between the TM1 segment and the downstream Pcp1 cleavage site in Mgm1 WT (Figure 12). For the generation of *s*-Mgm1 in Mgm1 WT, the TM1 segment is translocated through a pore formed by the TIM23 complex, thus Mgm1 WT with the hydrophilic domain extension could serve as a control for the membrane dislocation through a proteinaceous environment. Here, the relative ratio of *s*-Mgm1 to *l*-Mgm1 was unaffected by the presence of 24, 50 or 105 amino acid long hydrophilic segment, demonstrating that addition of hydrophilic moiety between the two TM domains did not interfere with translocation/insertion efficiency of Mgm1 through the TIM23 complex (Figure 12). Further, this result showed that presence of long hydrophilic moiety in the upstream of the rhomboid cleavage site did not impair cleavage efficiency of Pcp1.

Taken together, these results suggest that the *m*-AAA protease is incapable of dislocating a large hydrophilic domain across the IM, subsequently implicating that

the membrane dislocation probably occurs through the lipid membrane environment.

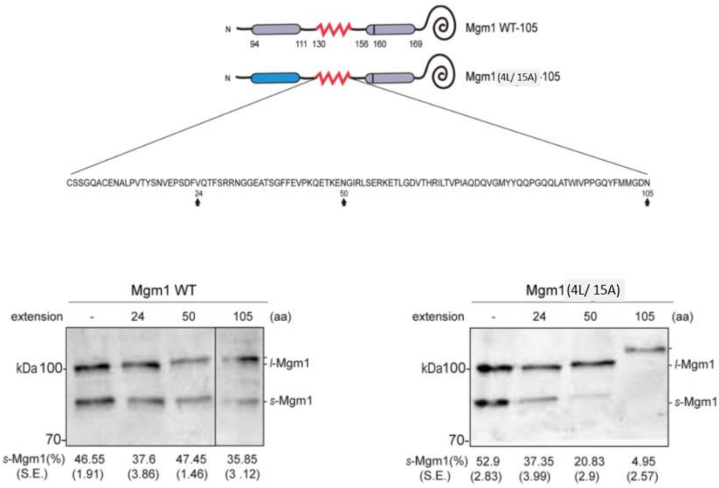

Figure 12. Dislocation of a TM segment with a large hydrophilic IMS moiety is impaired. A, schematic of Mgm1 WT and Mgm1(4L/ 15A) with a hydrophilic stretch. A soluble periplasmic (P2) domain from E. coli was added in between residues 130 and 131 of Mgm1 at the lengths of 24, 50, and 105 amino acids. The inserted amino acid sequence is shown, with arrows pointing toward the site of truncation. The Pcp1 cleavage site of Mgm1(residue 160) is indicated by a black line in TM2. B, dislocation efficiency of Mgm1WT and Mgm1(4L/ 15A) with 24-, 50-, or 105-amino acid extensions. Yeast transformants expressing Mgm1(*left*) or Mgm1(4L/ 15A) (*right*) with 24-, 50-, or 105- amino acid extensions were lysed and analyzed as described in Figure 9. Relative amounts of *s*-Mgm1 quantified from three independent experiments are indicated at the bottom with standard errors (S.E).

3. Discussion

The TM domains of the *m*-AAA complex are shown to be indispensable for membrane protein degradation [13], but their function on dislocating proteins out of the IM is poorly understood. By replacing each TM at a time, the presented data showed that the replacing of TM2 in Yta10 and Yta12 caused defects in dislocation of substrate proteins.

However, the replacement of TM2 of Yta10/12 exhibited different defects in protein dislocation. Replacement of TM2 of Yta10 impaired the dislocation of Mgm1(L/A) variants only, whereas replacement of TM2 of Yta12 showed defects in the dislocation of all tested substrates. The general impairment in protein dislocation observed with TM2 replacement of Yta12 was unexpected, because the dislocation and subsequent maturation of Ccp1 was shown to be unaffected in the Yta12 mutant strain lacking both TM domains [13]. Therefore, it is less likely that the TM2 of Yta12 is indispensable for membrane protein dislocation or substrate recognition. Augustin et al. [7] have shown that coordinated inter-subunit signaling between AAA domains of Yta12 and Yta10 is critical for dislocation of Ccp1. If the TM2 replacement causes subtle misalignment between the AAA domains of Yta12 and Yta10, then it could impair ATP hydrolysis, and then subsequent membrane dislocation. However, in the absence of entire TM domains, the AAA domain of Yta12 could be better positioned by interaction with the AAA domain of Yta10. On the other hand, Yta10 TM2 replacement selectively impaired the dislocation of Mgm1(nL/ (19-n)A) constructs while Ccp1 and Cox5aT-MFP variants were still dislocated well in the Yta10 TM2 deletion mutant, meaning that the dislocation function itself is not impaired. Thus, these results imply that replacement of TM2 of Yta10 likely causes impairment in the process of selective substrate recognition.

Because Yta10 and Yta12 share high sequence homology (Figure 13), at present we cannot exclude the possibility that TM2 of Yta10 and Yta12 has a redundant function in the recognition of membrane substrates. Although most substrates need one or the other, for some substrates, such as Mgm1(nL/ (19-n)A), require both. In the case of the *i*-AAA protease Yme1, it has been shown that both N- and C-terminal helical domains serve to recognize different degradation substrates [25-28]. Given that the *m*-AAA protease plays a diverse role in mitochondrial proteostasis, it would not be surprising if it has multiple modes of substrate recognition.

Next, we probed the length of the hydrophilic polypeptides that the *m*-AAA protease can dislocate from the membrane by introducing different lengths of hydrophilic stretches in the *m*-AAA protease substrate. Our results show that the dislocation efficiency is decreased significantly as the hydrophilic extension

lengthens. If the dislocation occurs in a proteinaceous pore, then it would be less sensitive to the length of the hydrophilic moiety; however, if the dislocation occurs in the lipid membrane, then the presence of a long hydrophilic segment would be energetically unfavorable. Hence, these results implicate that the *m*-AAA protease dislocates the TM domain from the lipid environment and that it would be incapable of dislocating a large IMS domain across the membrane. It can be assumed that, for the *m*-AAA protease to extract IM proteins for degradation in the matrix, either the IMS domain should be small or cleaved off by corroborating with other proteases prior to extraction from the membrane.

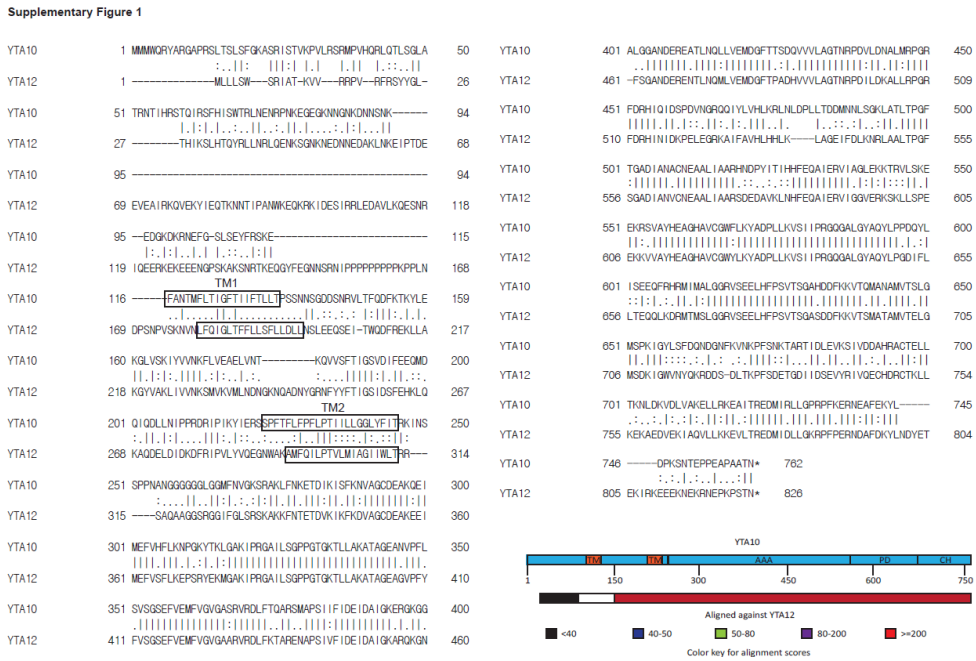

Figure 13. Yta10 and Yta12 share high sequence homology.

4. Materials and Methods

Yeast strains

W303-1a (*MATa, ade2, can1, his3, leu2, trp1,* and *ura3*) was used as a parental strain in this study. *yta10*Δ (*MATa, ade2, can1, his3, leu2, trp1, ura3, yta10::HIS3MX6*) was made by standard homologous recombination, substituting *YTA10* with an amplified *HIS3MX6* [29]. The primers used for the amplification of HIS3MX6 cassette were 5' CAGCGTTTGCAGACGTTATCTCGGATCCCCGGGTTAATTAA 3' and 5' TTGGGTAGAACGGTGTATTGTGTTGAATTCGAGCTCGTTTAAAC 3'. yta10Δ was used to make *yta10*Δ*yta12*Δ (*MATa, ade2, can1, his3, leu2, trp1, ura3, yta10:: HIS3MX6, yta12::KanMX6*) by substituting *YTA12* with *KanMX6*. The primers used for the amplification of *KanMX6* cassette were 5' TATCGGTTCGTTCAATAAGAAAGTC 3' and 5' GCCCTTAAGATGACCTACGTTTATT 3'. These yeast strains were cultured at 30°C in this study.

Plasmid construction

YTA10 was amplified from the genomic DNA with using a set of primers; 5' ATAGGGCGAATTGGAGCTCCACCGCGGTGGCGTTGTACATATATCTGCT 3' and 5' TATCGATAAGCTTGATATCGAATTCCTGCAGGATTTAATAAATGAAGGTGTT 3'. *YTA12* was amplified from the genomic DNA of using a set of primers 5' GGTGGCGGCCGCTCTAGAACTAGTGGATCCACAGCGCGATACAATTTTC 3' and 5' ATCGATAAGCTTGATATCGAATTCCTGCAGAGGGAGTAGATTTGAAGTCTC 3'.

The set of primers amplified *YTA10* and *YTA12* with 1Kb upstream sequences and 500bp downstream sequences to include endogenous promoters and potential transcriptional regulators, and contained nucleotides for cloning the amplified product into pRS314 or pRS316 respectively by homologous recombination [pRS314 *YTA10* WT], [pRS316 *YTA12* WT]). TMs of Yta10 were replaced with a TM of Mdl2 using [pRS314 *YTA10* WT] as template for site directed mutagenesis. Two sets of primers used to replace TMs of Yta10 were 5' TTAACCATATCATGTTCCATAGGCATGTCTTCCAGTAACAACTCAGGAGAC 3' with 5'

AAGAAGTATGGCTGTAAGAAGCAGTTTCCAATCTTCCTTAGATCTGAAGTATTCTGATAA 3' and 5'GCTGCTAATTTTGGTAGATTTATATTATTGAGAAAAATAAATAGTTCACCACCA3' with 5' ACAACCAATCAGTAAAGCAACAGTAAAAAAGGAAGAAGATCTCTCAATGTATTTGATG 3', each used to replace TM1 domain and TM2 domain of Yta10 with a TM domain of Mdl2, respectively. In the same manner, 5' TTAACCATATCATGTTCCATAGGCATGTCTAACAGTTTGGAAGAGCAAAGTG 3' with 5' AAGAAGTATGGCTGTAAGAAGCAGTTTCCAATCGTTAACATTTTTCGATACAGGATTACT 3' and 5' GCTGCTAATTTTGGTAGATTTATATTATTGCAAGAAGATCGGCACAAGC 3' with 5' ACAACCAATCAGTAAAGCAACAGTAAAAAAGGATTTAGCCCAATTGCCTTCTTG 3' were used to replace TM1 domain and TM2 domain of Yta12 with a TM domain of Mdl2 using [pRS316 YTA12 WT] as a template for site directed mutagenesis.

Mgm1, Ccp1 and Cox5aT model proteins used in the previous studies were adopted. To make Mgm1 with a P2 domain inserted between the residues 130 and 131 of Mgm1 WT and Mgm1(nL/ (19-n)A), overlap PCR was performed. First, N-terminal part of Mgm1WT and Mgm1(nL/ (19-n)A) were amplified using 5' TGTTACGCATGCAAGCTTGATATCGAAATGAGTAATTCTACTTCATTAAGG 3' and 5' TAAATCCTTGATTCGATCTAGTTT3'. C-terminal part of Mgm1WT were amplified using 5' GGTGAATCGATGAAGGAAAAG 3' and 5' TTAGAGAGCGTAATCTGGAAC 3'.

P2 domain was amplified from LepH2 protein using primers, 5' AAACTAGATCGAATCAAGGATTTATGCAGTTCCGGCCAG3' in combination with 5'CTTTTCCTTCATCGATTCACCAACGAAATCGCTCGGTTC3'or 5'CTTTTCCTTCATCGATTCACCATTTTCTTTGGTTTCCTGTTT3' or 5'CTTTTCCTTCATCGATTCACCGTTGTCGCCCATCATGAA3' to generate different lengths of hydrophilic P2 stretches.

The N-terminal part of Mgm1WT and Mgm1(4L/ 15A) were each fused to P2 domain by overlap PCR, and the stitched products were further annealed to the C-terminal part of Mgm1 WT. The resulting PCR product was cloned into pHP84HA plasmid by homologous recombination.

Growth assay

*yta10*Δ expressing [pRS314 *YTA10* variants] were cultured in –Trp(Glucose) media overnight at 30°C. The overnight culture was diluted to 0.1 OD_{600} and cultured to 0.5 OD_{600} at 30°C. 10µl of culture was spotted on YPD or YPEG (Ethanol/Glycerol) plate and further incubated for two days at 30°C. Photos were taken on Chemi-doc-XRS+ system using epi light (Bio-rad).

*yta10*Δ/*yta12*Δ [pRS314 *YTA10* WT] expressing [pRS316 *YTA12* variants] were cultured in –Trp –Ura (Glucose) media overnight at 30°C. The overnight culture was diluted to 0.1 OD_{600} and cultured to 0.5 OD_{600} at 30°C. 10µl of culture was spotted on YPD or YPEG (Ethanol/Glycerol) plate and further incubated for two days at 30°C. Photos were taken on Chemi-doc-XRS+ system using epi light (Bio-rad).

Protein preparation and Western blotting

Preparation of lysates, SDS-PAGE and Western blotting were conducted as previously described [23]. Briefly, yeast transformants were grown overnight in 5 ml of SD media at 30 °C. Proteins were precipitated from 1 $OD._{600}$ unit of yeast cells by addition of trichloroacetic acid (TCA, Sigma). Precipitated proteins were resuspended in 40µl of sample buffer and incubated for 5 min at 95°C prior to SDS-PAGE. The samples were separated on 6.5% or 12.5% Tris-HCl gels (Bio-rad) and followed by Western blotting. Membranes were immunodecorated with an anti-HA antibody (Covance) and developed with Amersham Bioscience Advanced ECL kit on a Chemi-doc-XRS+ system (Bio-rad). Quantification of detected bands was done using Image Lab 5.0 (Bio-rad).

MrpL32 processing assay

From overnight cell cultures of *yta10*Δ expressing [pRS314 *YTA10* variants] and *yta10*Δ/*yta12*Δ [pRS314 *YTA10* WT] expressing [pRS316 *YTA12* variants], whole cell lysates were prepared by resuspending cells in the sample buffer (50mM Tris-HCl, 5% SDS, 5% Glycerol, 50mM DTT, 5mM EDTA, protease inhibitor cocktail (Leupeptin, Pepstatin A, Chymostatin, Benzamidine, Pefabloc, Aprotinin, Antipain), and bromophenol blue) and heating for 15 min at 60°C. Prior to gel loading, the samples were centrifuged at 14,000rpm for 5 minutes and the supernatant fractions were loaded onto 15% Tris-HCl gels (Bio-rad). The gel was run and developed as described in Protein preparation and Western blotting section with α-MrpL32

antiserum.

CHAPTER 2.

The Mgr2 regulates membrane insertion of marginal stop-transfer signals in the IM

2. 1. Introduction

The TIM23 complex

The TIM23 complex is a translocase for precursors containing the N-terminally located mitochondrial targeting sequence (MTS) in the mitochondrial inner membrane [30-32]. The complex is composed of Tim23/17/21/44/50, Pam16/17/18 and Mgr2 (Figure 14) [33].

Tim23 is a central component for the TIM23 complex and Tim17 is a homolog of Tim23 [34-37]. Tim23 and Tim17 along with Tim50 form the TIM23-core complex [38-44]. Tim23 and Tim17 have been cross-linked to precursor proteins [45]. Tim21 is anchored to the IM and exposes its C terminus to the IMS and interacts with the IMS domain of Tom22 of the TOM complex [35]. The TIM23 complex with Tim21 forms the $TIM23^{SORT}$ complex, which is in charge of lateral release of TM domains of precursor proteins into the IM [46, 47].

Tim50 is a main receptor for precursors destined to the matrix. It has a large IMS domain and recognizes MTS of precursors [38-44]. Tim44 is peripherally associated with the TIM23 complex and resides in the matrix. Tim44 acts as a scaffold protein for mtHsp70 [48-51]. Tim44, mtHsp70, and the presequence translocase-associated motor (Pam) 16/18 together are associated with the TIM23 complex and control the import motor activity, TIM23motor. Pam17 has a role on precursor translocation [35, 52-54]. Mgr2 is suggested to function as a gatekeeper for the insertion of IM proteins into the IM through the TIM23 complex [33, 55-58].

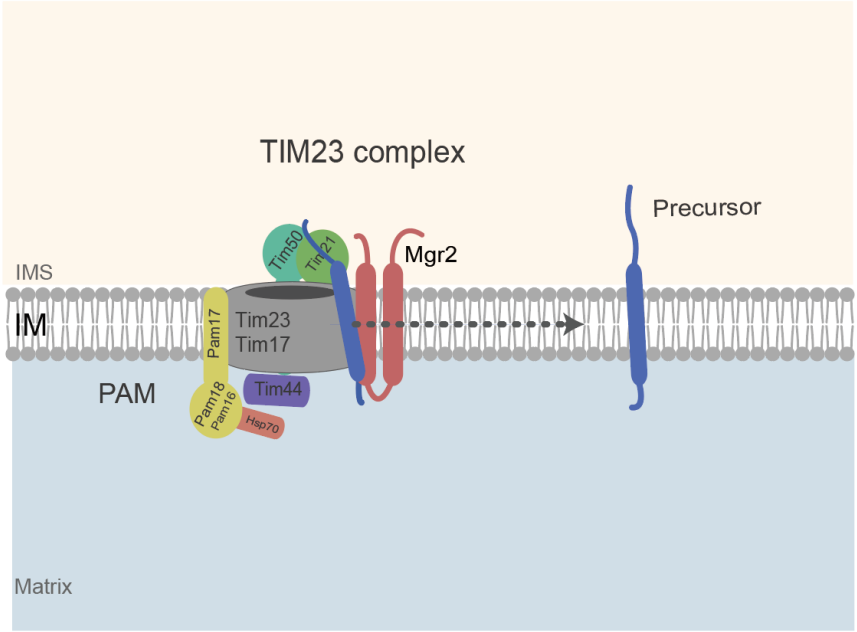

Figure 14. TIM23 complex is composed of several subunits. Tim17, 23 form channel pore, Tim21, 50 act as a receptor, Pam16, 17, 18 has s role for motor, and Mgr2 is a gatekeeper for precursor.

Mgr2, gatekeeper of a TIM23 complex

Mgr2 is directly associated with the TIM23 complex and forms the $TIM23^{SORT}$ [55]. It has two TMs and the first TM is shown to be responsible for the interaction with Tim23 and Tim21. The second TM of Mgr2 connects the TIM23 complex with the respiratory chain complex [33, 58].

Mgr2 has been suggested to regulate the lateral release for the IM-directed precursors by interacting with precursors residing in the TIM23 complex. In the Mgr2 overexpression condition, membrane insertion of the precursor is delayed while when Mgr2 is defective, membrane insertion is promoted (Figure15). A TM domain with defective membrane sorting signal was translocated into the matrix, but, in the absence of Mgr2, it was released to the IM [55]. In spite of the studies on Mgr2, the systematic characterization in the Mgr2 precursors remains to be done.

To assess the effects of Mgr2 on the TIM23-mediated membrane insertion, membrane insertion efficiencies was measured by a set of Mgm1 variants carrying a model TM helix with mutations in the flanking charged residues or composed of 19 L/ A residues instead of the original first TM domain of Mgm1.

Stop- transfer signal

The N-terminally targeted mitochondrial IM proteins is sorted at the level of the TIM23 complex. Whether these proteins follow the stop-transfer pathway or are conservatively sorted to the IM, depends on the determinants that the TIM23 complex uses to distinguish between domains that are “arrested” in the IM or “translocated” across to the matrix [59]. For these sorting pathways, the determinants have been identified: laterally sorted precursors have more hydrophobic than conservatively sorted one; downstream charges of the TM segment are important for insertion into the IM; proline residues are typically absent in arrested TM domain, but present in conservatively sorted [60]; the positive- inside rule is in the proteins that follow the conservative sorting pathway, used by the TIM23 complex [61]. It is important that the stop-transfer and the conservative sorting pathways are not mutually exclusive [62].

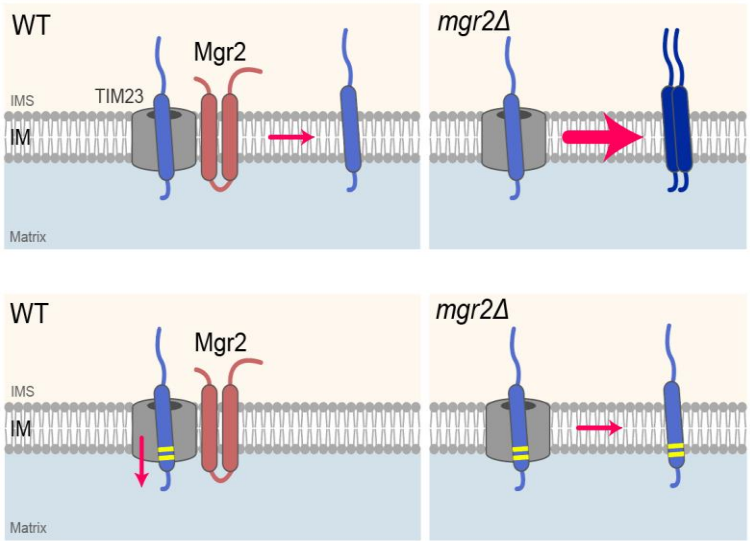

Figure 15. Membrane protein insertion is facilitated, when Mgr2 is absent. When the sorting signal is defective, protein is translocated. However, Mgr2 is absent, protein can be inserted into the IM.

This study aimed to define the characteristic of TM and its flanking residues, which are recognized by the Mgr2, in membrane protein insertion (Figure 16). I expect that understanding membrane inserted protein into the mitochondrial IM.

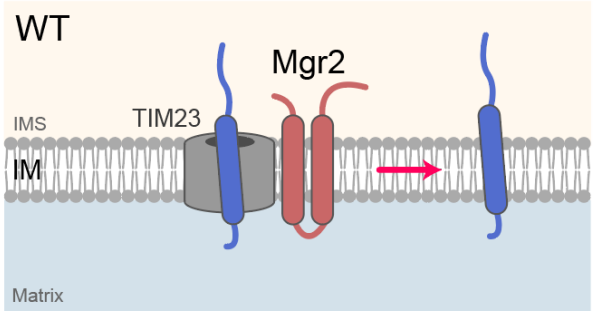

Figure 16. Mgr2 is proposed as a gatekeeper in IM. Mgr2 is proposed to gatekeeping role for the TM containing role in TIM23 complex.

2. 2. Results

2. 2. 1. Mgm1, as a Mgr2 substrate

It has been shown that Mgr2 makes extensive contacts with both the hydrophobic region and the matrix-facing positively charged residues of a stop transfer signal. However, a systematic dissection for these features that Mgr2 helps to recognize prior to IM sorting has not yet been conducted. To perform this analysis, we introduced Mgm1 as a tool, which has the dual topology. *s*-Mgm1 is generated when TM1—containing a stop-transfer signal—is translocated across the IM and the downstream rhomboid cleavage site in TM2 is processed by Pcp1 in the IM (Figure 6). Due to the unique characteristics of Mgm1, generating membrane-inserted long form and translocated-cleaved short form, Mgm1 constructs have been useful to assess the effects of Mgr2 on regulation of protein insertion into the IM. Moreover, Mgm1 with the hydrophobic TM domain being at the threshold of membrane insertion efficiency by the TIM23 complex, can also be a good tool for investigating the function of Mgr2.

2. 2. 2. Threshold hydrophobicity for the TM helix insertion is shifted by deletion of Mgr2

When TM1 of Mgm1 was replaced by a set of 19 amino acid stretches composed of n leucines and (19-n) alanines (Mgm1 (nL/ (19-n)A)) constructs (Figure 17), the relative amounts of *l*-Mgm1 and *s*-Mgm1 produced positively correlated with the hydrophobicity of the TM1 segments: the higher the hydrophobicity, the higher the fraction of *l*-Mgm1 in the WT strain [55].

To systematically assess the effects of Mgr2 on the TIM23 complex-mediated TM helix insertion into the IM, we analyzed membrane insertion efficiencies of Mgm1 (nL/ (19-n)A) variants in Mgr2 deletion and Mgr2 overexpression (↑) strains relative to the isogenic WT strain. Mgm1 (nL/ (19-n)A) constructs were expressed in the WT, *mgr2*Δ and Mgr2↑ strains. Whole cell lysates were prepared from these strains and the relative amounts of *l*-Mgm1 in each strain were assessed by SDS-PAGE and Western blotting (Figure 18).

Compared to the isogenic WT strain, membrane insertion efficiencies of Mgm1 variants carrying a moderately hydrophobic segment (5L/14A, and 6L/13A) were significantly enhanced in the absence of Mgr2. Membrane sorting of less hydrophobic (3L/16A and 4L/15A) or more hydrophobic segments (7L/12A and

8L/11A) were minimally or not affected by Mgr2 deletion. For the 5L/14A Mgm1, reduced level of *l*-Mgm1 was detected upon Mgr2 overexpression, suggesting that membrane insertion of this range of hydrophobicity is especially sensitive to Mgr2.

Overexpression of Mgr2 exhibited more complex effect, resulting in subtle enhanced membrane insertion of less hydrophobic segments (3L/16A, 4L/15A), decreased membrane insertion of moderately hydrophobic segment (5L/14A), and very hydrophobic TM domains (7L/12A, 8L/11A) were not affected by. Hence, it is difficult to conclude the effects of overexpression of Mgr2 with these test Mgm1 TMs. Since Mgr2 facilitates TOM- TIM supercomplex tethering [47], it remains to be determined whether the formation of TOM-TIM supercomplex is modulated depending on copy number of Mgr2 and/or different types of the incoming hydrophobic segments.

In terms of 50% membrane insertion (*i.e.* threshold hydrophobicity), in the WT strain, it was at n = ~ 5- 6 leucines, but when Mgr2 is absent, the number of leucines required was decreased to n= ~ 4- 5. Increase of the TM helix insertion efficiency in the Mgr2 deletion for the threshold hydrophobic TM domains was especially notable. These results suggest that Mgr2 fine-tunes membrane insertion of moderately hydrophobic segments through the TIM23 complex into the IM.

WT	VITRRSISHFPKIISKIIRLPIYVGGGMAAAGSYIAYKMEEA
nL/(19-n)A	LSETSGGPGAAAAAAAAAAAAAAAAAAAGPGGVPGQQ
3L/16A	AAAALAAAALAAAALAAAA
4L/15A	AAAALALAAAAALALAAAA
5L/14A	AAAALALAALAALALAAAA
6L/13A	AAAAAAALLLLLLAAAAAA
7L/12A	AAAAAALLLLLLLAAAAAA
8L/11A	AAAAAALLLLLLLLAAAAA

Figure 17. Mgm1 constructs are used in this study. Mgm1, sequences of and surrounding TM1 are shown. The underlined Mgm1 residues were replaced with nL/(19-n)A segments listed below.

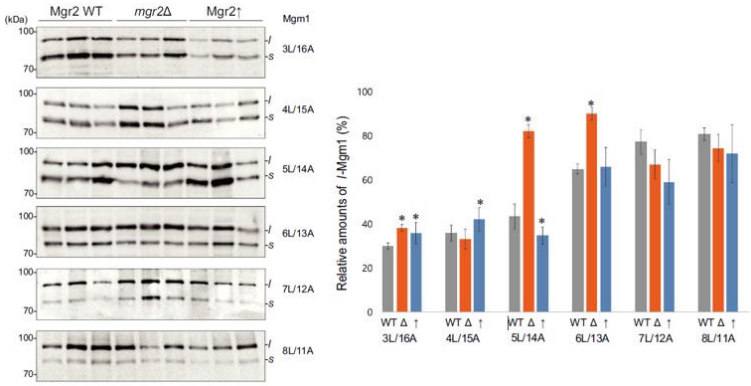

Figure 18. Membrane insertion efficiency of Mgm1 (L/A) variants is modulated by Mgr2. (*left*) Whole-cell lysates of Mgr2-WT (WT), -deletion (Δ), or -overexpression (↑) cells expressing Mgm1 (nL/(19-n)A) constructs were analyzed by SDS/PAGE and western blotting with an a-HA antibody. *l*-Mgm1 (l) and *s*-Mgm1 (s) bands are labeled. Each construct was tested at least three times independently. (*right*) Relative amounts of l-Mgm1 of Mgm1 (L/A) variants in Mgr2-WT, -deletion (Δ), and -overexpression (↑) cells were quantified from (A) using IMAGE LAB (Bio-Rad) and plotted. A t-test was performed to check the statistical significance of the observed differences relative to the WT strain. * Marks samples with $P < 0.05$.

2. 2. 3. Effects of charged flanking residues on membrane insertion of Mgm1 in the mgr2Δ and Mgr2↑ strains

TM1 of Mgm1 is unique in that it is only inefficiently inserted into the IM by the TIM23 complex. It has been shown that not only the hydrophobicity of the TM helix but flanking charged residues are important for this dual-sorting.

To determine how Mgr2 affects membrane insertion of Mgm1 TM1 via flanking charged residues (Figure 19), Mgm1 variants with mutated charged flanking residues were expressed in *mgr2*Δ, Mgr2↑ and WT strains (Figure 20).

For Mgm1 WT, membrane sorting of Mgm1 was increased in Mgr2 deletion (*mgr2*Δ) whereas decreased in overexpression (Mgr2↑) strain as previously observed (Figure 20) [55].

It has been shown that replacing the N-terminal positively charged residues flanking TM1 on the matrix-side (Mgm1 R78A, and R79A) significantly decreased the membrane insertion efficiency of Mgm1 in the WT strain.

Because membrane insertion efficiency was much reduced for these constructs, additional reduction in membrane insertion could be difficult to measure in the mgr2Δ or Mgr2↑ strains. So, we used the Mgm1 RR78,79AA construct, which was made more hydrophobic by replacing three amino acids within TM1 (GGM to VVL mutation). The Mgm1 variant carrying GGM:VVL showed no difference between three Mgr2 strains (data not shown). When this variant was expressed and assessed, its membrane insertion efficiency, the fraction of *l*-Mgm1 was shown increased in the absence of Mgr2 (Figure 20).

Next, membrane sorting of the Mgm1 variants carrying mutated negatively charged flanking residues at the IMS-side C-terminal end of the TM1 was assessed. When two negatively charged Glu residues at the end of TM1 were mutated to alanines (Mgm1 E114A, 115 AA), the membrane insertion efficiency was slightly increased in the *mgr2*Δ strain (Figure 20).

Taken together, membrane insertion efficiency was increased in Mgr2 deletion strain for the Mgm1 charge variants (R78A, RR78,79AA, RR78,79AA GGM: VVL, and EE114,15AA), suggesting that flanking charged residues may be important determinants for the Mgr2-mediated membrane sorting of the TM domains.

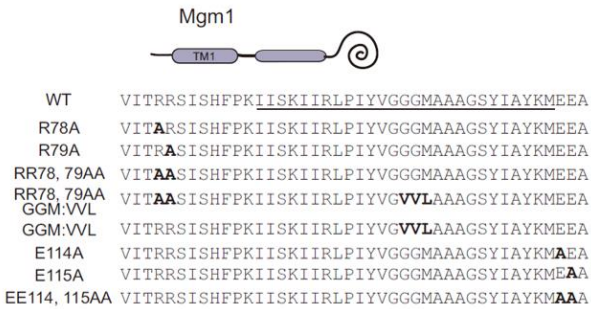

Figure 19. Mgm1 constructs are used in this study. Mgm1, sequences of and surrounding TM1 are shown. Mgm1 with mutated charged residues are indicated in bold.

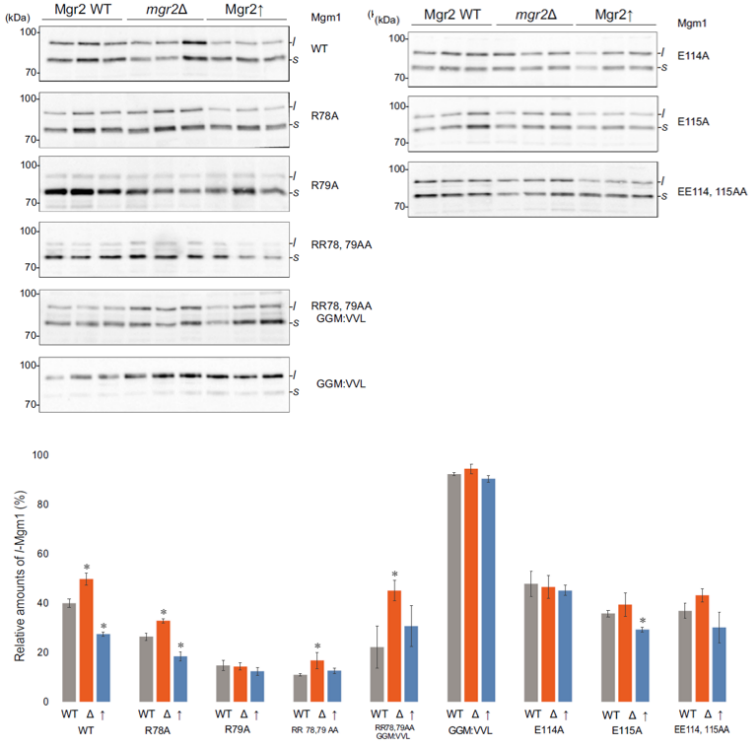

Figure 20. Effects of Mgr2 on membrane insertion of Mgm1 via charged flanking residues. (*upper*) Whole-cell lysates of Mgr2 WT, mgr2Δ, or Mgr2↑ cells expressing Mgm1 WT or variants with mutated flanking charged residues were analyzed. (*lower*) Relative amounts of l-Mgm1 of Mgm1 variants in Mgr2-WT, -deletion (mgr2Δ), and -overexpression (Mgr2↑) cells were quantified from (*upper*) using Image Lab (Bio-Rad) and plotted. $P < 0.05$, denoted as *.

2. 3. Discussion

Taken together, these results suggest that Mgr2 is critical for regulating membrane insertion efficiency of precursor proteins with the threshold hydrophobicity and matrix-facing positively charged residues flanking residues.

A role of the Mgr2 for the membrane protein sorting has been proposed; however, the factors in Mgr2 substrates that are discriminated by Mgr2 during membrane sorting were poorly understood. A systematic quantitative assessment of IM sorting of sto*p*-transfer signals in model precursor proteins revealed how Mgr2 acts on protein sorting of hydrophobic segments in the IM. Threshold hydrophobicity for the TIM23-mediated membrane insertion of Mgm1 variants is decreased in the absence of Mgr2, suggesting that hydrophobic partitioning into the IM is facilitated in the absence of Mgr2. However, the membrane insertion of test hydrophobic segments was not linearly increased in the range of hydrophobicity, but the effects of Mgr2 were pronounced for the marginally hydrophobic TM. Consistently, Mgr2 was reported to influence membrane sorting of the TM domain of Cyb2 which is moderately hydrophobic. We also showed that the proteins lack the matrix-facing positively charged amino acids were less efficiently inserted into the membrane. However, increased hydrophobicity in sto*p*-transfer signal allowed proteins without those matrix-facing positively charged amino acids to be efficiently released to the IM in the absence of Mgr2. It showed that the hydrophobicity of sto*p*-transfer signal and flanking positively charged amino acids are critical factors for Mgr2-dependent regulation of membrane proteins sorting into the IM.

We suggest that strong or weak stop-transfer signals are likely to be quickly equilibrated to the membrane or to the matrix, whereas moderate sto*p*-transfer signals linger between the lipid membrane and the protein channel relatively longer. A partial opening of the lateral gate in the absence of Mgr2 may have a major impact in membrane sorting of marginal stop-transfer signals.

2. 4. Material and Methods

Yeast strains and plasmids

The *Saccharomyces cerevisiae* wild-type (WT) YPH499 (*MATa, ade2, lys2, his3, leu2, trp1, ura3*), *mgr2*Δ (YPH499, *mgr2*::*KANMX6*) and Mgr2↑ (*mgr2*Δ [pPGK-*MGR2*]) were used in this study [3, 14-16] . The plasmids encoding Mgm1 variants in pHP84HA vector [1, 2, 11-13] were transformed into YPH499, *mgr2*Δ and Mgr2↑. Yeast transformants were cultured on –Leu (YPH499 and *mgr2*Δ) or –Leu –Ura (Mgr2↑) synthetic defined medium (0.67% Bacto yeast nitrogen base dropout amino acid mix, and 2% glucose or 0.67% Bacto yeast nitrogen base dropout amino acid mix, 3% glycerol, and 0.2% glucose) at 30°C.

Protein preparation, SDS-PAGE, and Western blotting

Yeast transformants expressing Mgm1 variants were cultured in 2 kinds of synthetic defined medium (0.67% Bacto yeast nitrogen base dropout amino acid mix, and 2% glucose or 0.67% Bacto yeast nitrogen base dropout amino acid mix, 3% glycerol, and 0.2% glucose) at 30°C overnight. Proteins were prepared as whole cell lysates [2] [12]. Whole cell lysates were prepared from a total 10 $O.D._{600}$ units of cells grown at $O.D._{600}$ 0.6-0.8. Cells were lysed by addition of 1X lysis buffer (50mM Tris-HCl pH 7.5, 5% SDS, 5% glycerol, 50mM DTT, 5mM EDTA, Bromophenol Blue, 2ug/mL Leupeptin, 2ug/mL Pepstatin A, 1ug/mL Chymostatin, 0.15mg/mL Benzamidine, 0.1mg/mL Pefabloc, 8.8ug/mL Aprotinin, 3ug/mL Antipain). Cell debris was removed by centrifugation at 14,000 rpm for 5 minutes. Cleared lysates were incubated at 55°C for 15 minutes prior to SDS-PAGE. The samples were separated on 6.5% Tris-HCl gels (Bio-rad) for Western blotting. Membranes were blotted with an anti-HA antibody (Covance) and developed with Lumigen ECL Ultra kit on a Chemi-doc-XRS+ system (Bio-rad). Quantification of detected bands was done using Image Lab 5.0 (Bio-rad). Relative amounts of l-Mgm1 are quantified as [*l*-Mgm1/ (*l*-Mgm1+ *s*-Mgm1)] x 100(%).

CHAPTER 3

Yta10 targeting factors are elucidated for the mitochondrial targeting *in vivo*

3. 1. Introduction

Protein targeting to mitochondria

Majority of the mitochondrial proteome is encoded from the nuclear genome and targeted to mitochondria. Their correct targeting to mitochondria is crucial for biogenesis of mitochondria and its function. For targeting to mitochondria, ~70% of mitochondrial proteins have N-terminal mitochondrial targeting sequence (MTS, also called presequence). MTS functions in targeting and importing of nuclear encoded proteins to the mitochondria as the signal sequences do for the proteins destined to the secretory pathway to the endoplasmic reticulum (ER) [63].

Post and Co-translational protein targeting to mitochondria

It has long been thought that mitochondrial proteins are post-translationally targeted. Studies have shown that longer presequence facilitates efficient translocation across the double membranes of mitochondria during post-translational translocation [64-66]. For example, a presequence of Su9, a precursor to the subunit 9 of *Neurospora crassa* F_0-ATPase is 69 residue long and contains two regions that bind to the major import receptor Tom20 [66]. While the second region still binds to Tom20, the first region is handed over from Tom20 to the intermembrane space part of the TOM complex, increasing protein import efficiency [66]. Another study has shown that a long presequence of Cytochrome b_2 (65 residue long) is grabbed by the matrix Hsp70 which facilitates unfolding of a mature domain for protein import into mitochondria [64, 65]. When the presequence was truncated, the import rate was decreased [64, 65]Hence, these studies suggest that long presequences ensure efficient and fast import of mitochondrial proteins during post-translational translocation. Also, cytosolic chaperones are known to be critical for targeting. Hsp40 family, also called J proteins Ydj1, Xdj1 and Sis1 in yeast, recognizes mitochondrial targeted precursors and recruits another cytosolic Hsp70 chaperones (Ssa1–Ssa4) [67-73]. Hsp90, Sti1, binds to precursors in the cytosol [74, 75]. These cytosolic chaperones have been suggested to maintain precursors in an unfolded import-competent state, and prevent aggregation in the cytosol.

Ribosome-proximity study has shown that mitochondrial inner membrane proteins, such as Oxa1 and Yta10, are co-translationally targeted into mitochondria [76]. Further, a subset of mitochondrial mRNAs is localized to the mitochondria via the 3' end untranslated region (3' UTR) which binds to Puf3, a RNA binding protein, and

translated at the mitochondria surface [77-85]. Yta10 has Puf3 binding element (PBE) in the 3' UTR. These studies, thus illustrate that Yta10 is co-translationally translocated and inserted into the mitochondrial inner membrane (Figure 21).

Nascent polypeptide-associated complex (NAC) is suggested to interact with cytosolic ribosomes [79, 86-88] and the mitochondrial OM protein, Om14, mediating targeting of cytosolic ribosomes to mitochondria [84]. Deletion of NAC leads to mis-localization of mitochondrial proteins to the ER [89].

The ER-mediated Mitochondrial Targeting (ER-SURF)

A pathway named ER surface-mediated mitochondrial protein targeting (ER-SURF) has been recently revealed [90]. In this pathway, some mitochondrial inner membrane proteins are localized to the ER membrane prior to their import into the mitochondria (Figure 22). The ER-resident J protein Djp1 is a key component, transporting ER-localized mitochondrial proteins from the ER to the Tom70 receptor in mitochondria [70, 90, 91]. Presumably, the ER membrane prevents misfolding of mitochondrial proteins, minimizing accumulation and aggregation of mitochondrial membrane protein precursors in the cytosol.

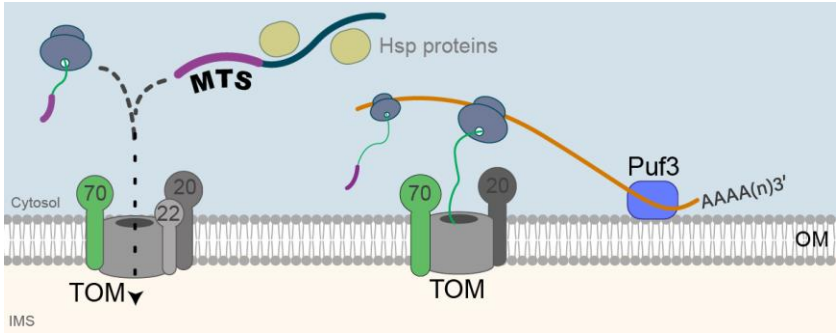

Figure 21. MTS and Puf3 binding element facilitate the protein targeting and localization. N' terminal located MTS is recognized by the TOM receptors. Puf3 binding element (PBE) is located in the 3' UTR, and recognized by the Puf3 in the OM surface.

Recognition of mitochondrial proteins at the mitochondrial OM

Upon targeting to the mitochondria, proteins engage with the TOM complex to pass across the OM. It is a 400 kDa large protein complex, containing three receptors, Tom20, Tom22, and Tom70, small proteins (Tom5, Tom6, and Tom7), and a central subunit, pore-forming Tom40 protein (Figure 21).

Tom20, via its cytosolic domain, binds to the hydrophobic face of the MTS. Tom22 transfers precursors to the Tom40 pore. Its negatively charged region binds to the MTS positively charged region with electrostatic interaction. Tom70 recognizes internal signals in carrier proteins [92] and internal MTS like signals (iMTS-Ls) [93]. Tetratricopeptide repeat (TPR) domain of Tom70 serves as an assistant to Hsp70 and Hsp90 during unfolding of precursors. Tom70 is also shown to be crosslinked with MTS, although Tom20 preferentially binds to the N-terminal MTS. Meanwhile it was reported that Tom20 and Tom70 are able to functionally replace with each other [94, 95].

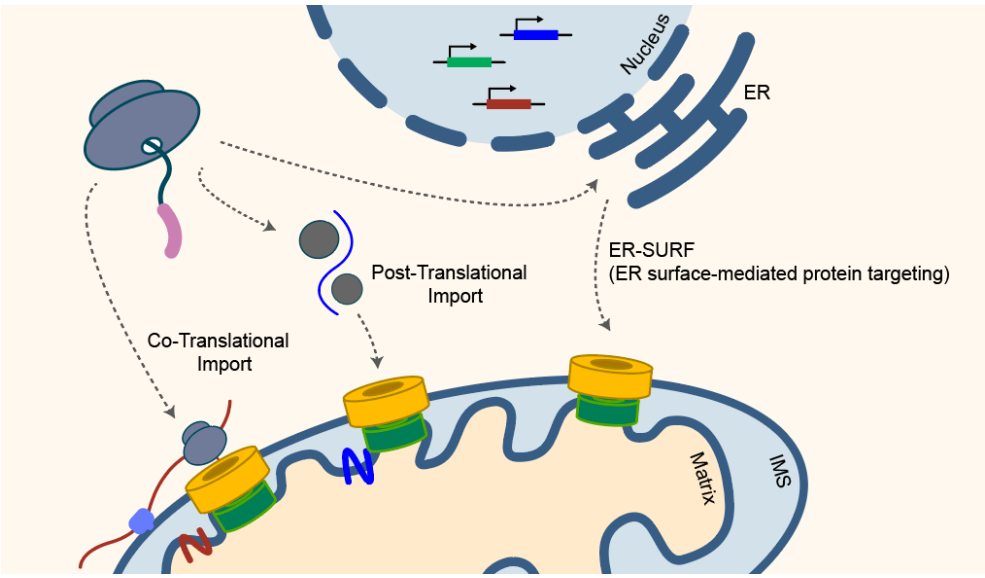

Figure 22. Mitochondrial precursors from cytosol are delivered in 3 ways. *(Middle)* In the post-translational translocation, precursor at the ribosome is completed, and cytosolic chaperones bind and protect from misfolding and aggregation. *(Left)*Certain mitochondrial proteins might be targeted co-translationally. In some cases, the mRNA-binding factor Puf3 on the mitochondrial surface facilitates this reaction. *(Right)* ER-mediated mitochondrial protein targeting: ER-SURF. Precursors bind where the ER J protein Djp1 recognizes the mitochondrial proteins. These proteins are handed over to the mitochondrial OM to be imported

Mitochondria targeting sequence (MTS)

MTSs are believed to form an amphiphilic α-helical structure with hydrophobic and positively charged/polar residues. The length ranges from 15 to 100 [96], with an average of 20 to 60 amino acids, and the average net charge in MTSs is +3 to +6 [97]. Once MTSs are imported in the matrix, it is cleaved by the mitochondrial processing peptidase (MPP). To identify the common characteristic of MTSs, N-proteome studies and MTS-prediction algorithms have been previously investigated. In spite of these studies and information on the common features of MTS, how these widely diverse characteristic of MTS is recognized by the general receptor and import machineries remains unclear.

It is unknown whether long presequence is required for co-translational import where unfolding of the mature domain is unnecessary. Likewise, it is poorly understood whether the Puf3 binding element (PBE) is essential for the co-translational import (Figure 21).

This thesis aimed to define the sequence elements essential for proper localization of Yta10 to the mitochondrial inner membrane. For that, presequence and the 3' UTR of Yta10 were systematically shortened, and assessed its import and membrane insertion by growth complementation, subcellular localization and fluorescence microscopy.

3. 2. Results

3. 2. 1. Characteristics of the Yta10 MTS

The MTS of Yta10 is predicted to be the residues 1 to 72 [98-100] or the residues 1 to 64 (Figure 23) [101]. MTS is cleaved by the MPP which cleaves at 1 residue downstream of Arg residue (R-2). Multiple cleavage sites are predicted in Yta10 MTS (Figure 23), and it is often difficult to know the MTS cleavage site as Arg is an abundant amino acid in MTS, and the MPP-cleaved protein can be further processed by Icp55 (one residue downstream after the MPP cleavage) or Oct1 (eight residue downstream after the MPP cleavage) [102].

Within the residues 1 to 72 of Yta10, negatively charged amino acids are absent and 16 positively charged amino acids are present which is more than the average charges of MTS (+3 to +6). Amphiphilicity was predicted to be present in the residues 3-15 and the Tom20 binding site was predicted to be present at the residues 3-8 (Figure 23).

Previous proteomics study identified the N terminus of the proteins from the isolated yeast mitochondria [102]. Yta10 is detected to have four different N-terminus; the 1st, 12th, 30th and 45th amino acids were detected as the N-terminal residue of Yta10 in the mitochondria. The uncleaved form (the 1st amino acid as the N-terminal residue) is likely the cytosolic precursor, probably bound to the cytosolic surface of the mitochondrial outer membrane whereas the other forms are presumed to be the mature forms that are cleaved by MPP, Icp55 and/or Oct1 in the matrix.

3. 2. 2. Defining the Yta10 MTS that is essential for its targeting to the mitochondria

As illustrated above, predictions nor the proteomics data define the targeting sequence which is required for Yta10 to be localized in the mitochondria. To experimentally determine the region of MTS that is critical for the mitochondrial targeting of Yta10, different regions of its MTS were serially truncated. The proteomics study has shown that the longest mature domain has the 12th residue at the N-terminus, implying that residues 1-11 may be a minimal MTS of Yta10 [102]. Hence, the MTS variant having 11 residues (Δ12-72), and serially longer MTS variants having 20, 31 and 63 residues (Δ21-72, Δ32-72, Δ64-72, Figure 25) were constructed.

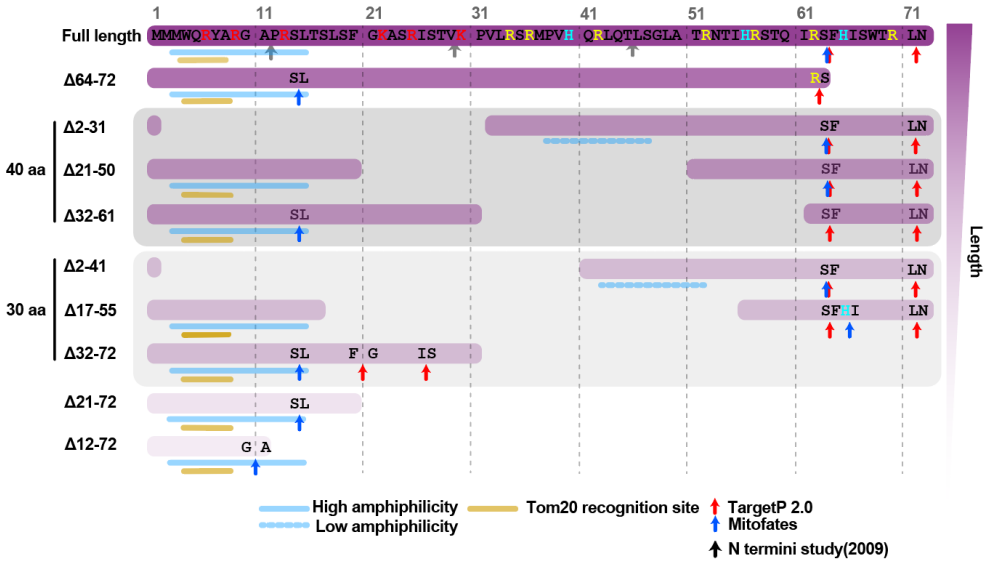

Figure 23. Yta10 FL and MTS variants are predicted for cleavage site, amphiphilicity, and Tom20 recognition site.

To assess proper targeting and membrane insertion into the mitochondrial inner membrane, I carried out in vivo growth complementation assay. Since Yta10 is essential for cellular respiration in mitochondria, exogenous expression and subsequent import into mitochondria is required for the *yta10* deletion cells to grow in respiratory growth condition. It means that cells would grow on the respiration medium only when Yta10 is properly targeted and membrane inserted in the inner membrane.

Yta10 MTS variants having varying length of MTS were constructed by including the Yta10 endogenous promoter containing 1kb of the 5' UTR and 500 bp of the 3' UTR, and the C-terminus was fused with FLAG tag for detection by Western blotting (Figure 24). These Yta10 MTS length variants were expressed in the *yta10* deletion strain and tested by growth complementation assay on respiratory conditions at four different temperatures. The cells expressing the Yta10 Δ12-72, Δ21-72 did not grow at all temperatures even though the protein was expressed (Figure 24). In the case of Yta10 Δ32-72, cells grew weakly at 35°C, exhibiting temperature sensitivity.

To further monitor Yta10 targeting in a different manner, subcellular fractionation of mitochondria was carried out. If Yta10 is targeted to the mitochondria, Yta10 would be protected from Proteinase K (PK) due to inaccessibility of PK inside of the mitochondria. Yta10 (FL) and Yta10 Δ64-72 were protected from PK digestion, indicating that they were correctly targeted to the mitochondria (Figure 25). Lastly, proper localization of Yta10-yEGFP was monitored by GFP fluorescence microscopy (Figure 26) [103]. These data show the first 31 residues are needed for targeting of Yta10 to the mitochondria.

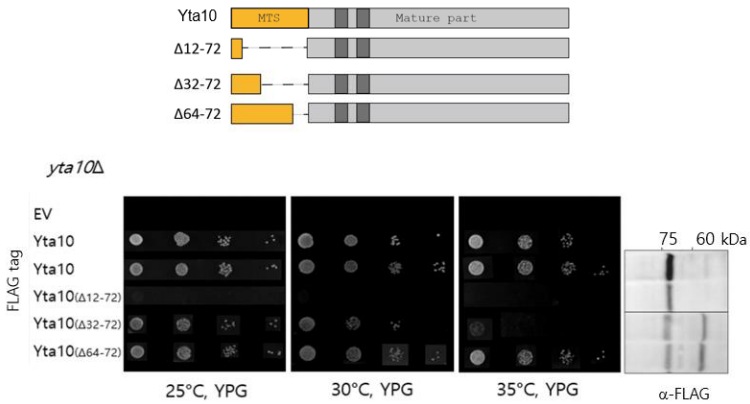

Figure 24. Yta10 MTS variants are monitored on targeting. (*Upper*) Yta10 MTS variants under the endogenous promoter were expressed in the *yta10*Δ strain, respectively. The transformants were cultured in glucose-containing liquid medium prior to spotting on YPG plates. The plates were incubated at 25, 30, 33, 35°C for 2 days prior to imaging. EV, empty vector; FL, Full length; Δ12-72, amino acid number 12 to 72 was deleted Yta10. (*Lower*) Cell expressing Yta10 MTS variants in the *yta10*Δ strain was harvested, lysed with TCA precipitation, subjected to SDS-PAGE and detected by Western blotting, and immunoblotted with α-FLAG antibody

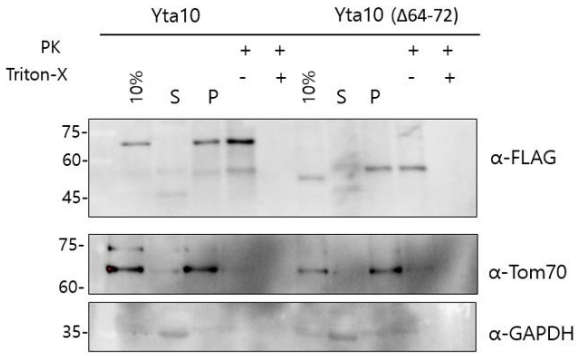

Figure 25. Yta10 FL and Δ64-72 was detected inside of the mitochondria. Yta10 FL and Δ64-72 expressed under the endogenous promoter in the *yta10*Δ strain, respectively. The transformants were cultured in a 30°C, glucose-containing liquid medium and shifted to glycerol-containing YPG medium. Yeast cells were subcellular fractionated, done SDS-PAGE and detected by Western blotting. Tom70 is control for membrane fraction and GAPDH is for cytosolic fraction.

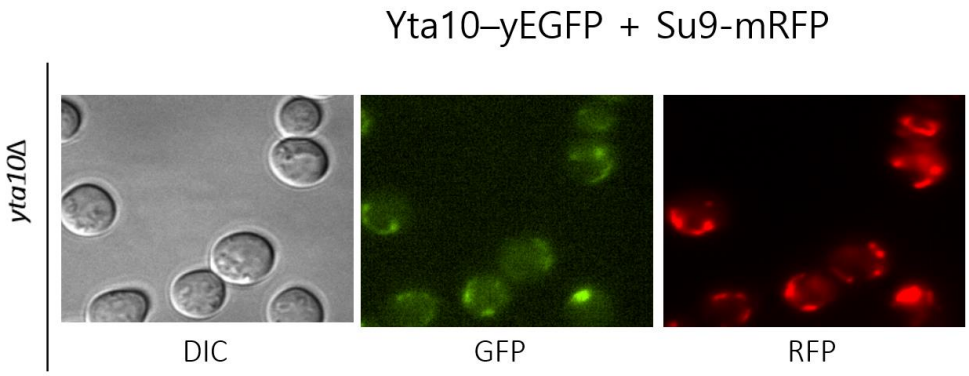

Figure 26. Yta10 is localized in mitochondria by fluorescence. Yta10-yEGFP construct was expressed under the endogenous promoter in the *yta10*Δ strain, and co-expressed with Su9-mRFP for mitochondrial marker. The transformants were cultured at 30°C in glucose-containing liquid medium prior to imaging. Cells were viewed with GFP and RFP filters

The N-terminal 72 residues were predicted to be the MTS of Yta10, therefore we wondered whether the C-terminal 40 residues could also function as MTS. For that, MTS Δ2-31 was constructed and its targeting was monitored by a growth complementation assay. Yta10 Δ2-31 complemented growth defects of the *yta10*Δ cells, indicating efficient mitochondrial targeting (Figure 27). These data show that within the predicted 72 residues of Yta10 MTS, the N-terminal 30 residues and the C-terminal 40 residues, both function as targeting signals for Yta10, suggesting that Yta10 MTS has tandem targeting signals.

Since the deletion of the N-terminal 30 residues did not affect the targeting of Yta10, we wondered whether the 30-residue deletions (MTS length 40 (L-40)) within the predicted 72 residues of Yta10 MTS also work as MTS. Constructs, Yta10 Δ21-50 that the middle 30 residues were deleted and Yta10 Δ32-61 that the C-terminal region were deleted were prepared and tested. The Yta10 Δ21-50 and Yta10 Δ32-61 were all complemented growth defects of *yta10* Δ cells, indicating that Yta10 MTS without 30 residues in any regions in its predicted MTS is functional (Figure 24). The Tom20 is the major import receptor for presequence containing precursors. Residues 3-11 were predicted to be Tom20 binding motif, but Yta10 Δ2-31 that lacks the Tom20 binding domain was efficiently targeted to the mitochondria, suggesting that binding to the Tom20 might not be essential for co-translational import of Yta10 *in vivo*.

Based on the observation that Yta10 MTS lacking the C-terminal 40 residues within the predicted MTS functions for mitochondrial targeting, I wondered whether 40 residue deletion within the predicted MTS functions as a targeting signal. Constructs carrying the MTS length lacking ~40 aa in the N-terminus (Yta10 Δ2-41) and in the middle (Yta10 Δ17-55) were constructed and tested (MTS length 30 (L-30)) (Figure 27). Yeast *yta10*Δ cells carrying Yta10 L-30 variants were all grown (Figure 27). The growth of these constructs was weaker without Tom70, and the Yta10 Δ32-72 showed the most severe growth defect in the absence of Tom70 (Figure 28). Tom70 is a receptor that binds to internal MTS like signals (iMTS-Ls) and TM domains of the inner membrane proteins [93]. It could be that residues between 32-72 of Yta10 might act as iMTS-Ls and bind to Tom70 during its import into mitochondria, facilitating import efficiency of Yta10.

One difference among the Yta10 L-30 is the number of positively charged residues: Yta10 Δ2-41 and Δ17-55 have 7 and 8 basic residues whereas Yta10 Δ32-72 has 6 (Figure 28). To check whether the difference of the number of positively charged amino acids affect the MTS function, one more positively charged residue was added or deleted from Yta10 Δ32-72. Ser27 was substituted to Arg to change the net

charge from 6+ to 7+. The Yta10 MTS Δ32-72, S27R, showed better growth complementation compared to Yta10 MTS Δ32-72, both in the presence and absence of Tom70. In comparison, the Yta10 MTS Δ32-72 R13A or K22A variant did not complement the growth defect of *yta10*Δ cells (Figure 28). These data show that at least 6 positively charged residues in the 30-residue long MTS are required for proper targeting of Yta10 to the mitochondria.

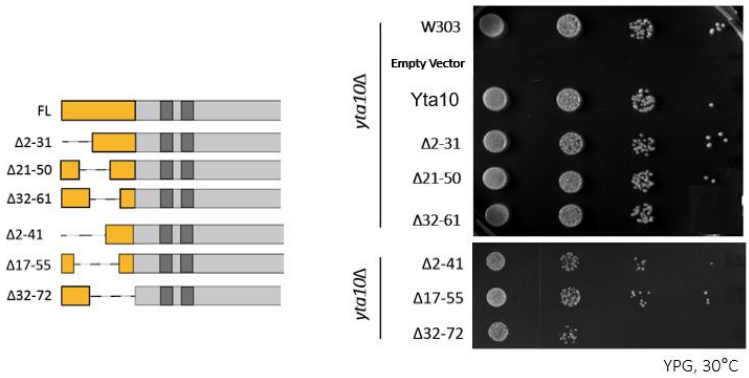

Figure 27. Yta10 MTS L-40 and L-30 variants were targeted to mitochondria. Yta10 MTS variants, under the endogenous promoter, were expressed in the *yta10*Δ strain, respectively. The transformants were cultured in glucose-containing liquid medium prior to spotting on YPD and YPG plates. The plates were incubated at 30°C for 2 days prior to imaging.

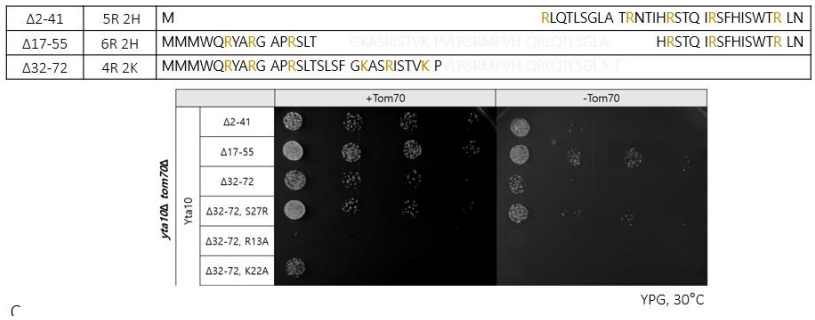

Figure 28. Basic charge residue alleviated the growth defect on Yta10 MTS L-30 variants. Yta10 MTS L-30 variants under the endogenous promoter were expressed in the *yta10*Δ/ *tom70*Δ strain, respectively. The transformants were cultured in glucose-containing liquid medium prior to spotting on YPD and YPG plates. The plates were incubated at 30°C for 2 days prior to imaging

3. 2. 3. Deletion of the Puf3 binding element did not affect targeting of Yta10.

A subset of mRNAs of mitochondrial proteins contains the Puf3 binding element (PBE) in the 3' UTR, downstream of the open reading frame (ORF) that binds to Puf3 in the OM and localized to the mitochondria. The 3' UTR region of Yta10 has a putative PBE at 102-111bp (CATGTATATA), and mRNA level of Yta10 was diminished in the puf3 deletion strain in previous genome-wide screening [104], implying that mRNA of Yta10 is potentially targeted by Puf3 to mitochondria. Whether the PBE is critical for Yta10 targeting, Yta10 variants without the PBE(ΔPBE) were prepared and expressed in the yta10 deletion strain and growth was assessed under respiratory conditions. For the Yta10 FL lacking the PBE, growth defects of yta10 deletion cells were completely rescued. In addition, Yta10 FL or Yta10 Δ32-72 lacking the PBE (Δ32-72, ΔPBE) also rescued the growth defect of the *yta10*Δ and *tom70*Δ double deletion strain (Figure 29). These results suggest that PBE alone does not affect the import of Yta10 to the mitochondria.

We accidentally prepared Yta10 FL without the 3' UTR (Yta10 3' UTR$\Delta_{1\text{-}500}$) (Figure 30). When the growth complementation assay was carried out with this construct, it did not complement the growth defect of yta10 deletion cells, indicating that Yta10 import is impaired without the 3' UTR (Figure 29). To check whether particular region of 3' UTR is important or sufficient length of the 3' UTR is needed for the Yta10 targeting to the mitochondria, Yta10 variants carrying the first 250bp (1-250) long and the last 250bp (251-500) of the 500bp 3'UTR, downstream of the Yta10 ORF were prepared (Figure 29). Expression of Yta10(3' UTR$\Delta_{251\text{-}500}$) restored the growth defect of the yta10 deletion cells whereas expression of Yta10(3' UTR$\Delta_{1\text{-}250}$) did not (Figure 29). When expression levels of the Yta10 variants having varying length of 3'UTR were assessed, Yta10(3' UTR$\Delta_{1\text{-}500}$) and Yta10(3' UTR$\Delta_{1\text{-}250}$) were not expressed (Figure 29). These data suggest that the first 250bp 3'UTR of Yta10 is essential for expression of Yta10.

In the previous figure, we assessed the targeting of Yta10 depending on different MTS and 3' UTR through the yeast growth complementation assay. To confirm previous results and further examine the targeting of Yta10 having varying MTS and 3' UTR region, Yta10 variants were fused with yeast enhanced green fluorescent protein (yEGFP) to monitor Yta10 targeting through fluorescence microscopy.

The localization of Yta10 FL-yEGFP including 500bp of the 3' UTR by GFP signal was overall merged with Su9-mRFP signal, a mitochondrial marker. But, Yta10 FL-yEGFP without 3' UTR (yEGFP 3' UTR$\Delta_{1\text{-}500}$) showed a diffused and weak GFP signal in cytosol, probably due to low protein expression (Figure 30).

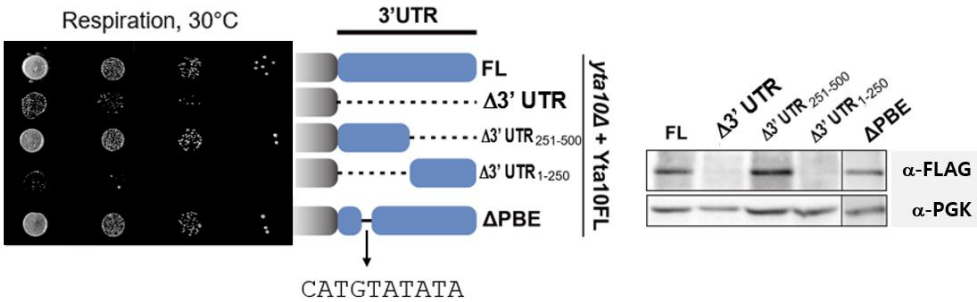

Figure 29. 3' UTR affects to Yta10 mitochondrial targeting. Yta10 UTR variants under the endogenous promoter were expressed in the *yta10*Δ strain, respectively. The transformants were cultured in glucose-containing liquid medium prior to spotting on YPD and YPG plates. The plates were incubated at 30°C for 2 days prior to imaging

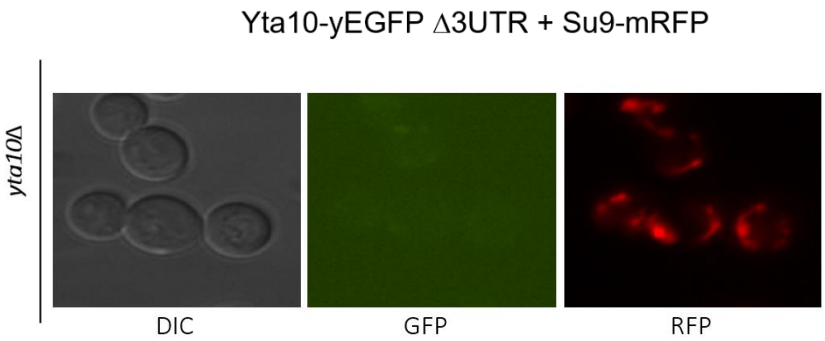

Figure 30. Yta10 was not localized in mitochondria, when 3' UTR is defective. Yta10 -yEGFP Δ3' UTR construct was expressed under the endogenous promoter in the *yta10*Δ strain, and co-expressed with Su9-mRFP for mitochondrial marker. The transformants were cultured at 30°C in glucose-containing liquid medium prior to imaging. Cells were viewed with GFP and RFP filters

3. 3. Discussion

In this study, I aimed to investigate effects of the length and the position in MTS and the PBE in 3' UTR of Yta10 on its targeting to mitochondria, using combined approaches of the *in vivo* growth complementation assay and subcellular fractionation in yeast. I found that while the PBE was not essential for the targeting of Yta10 to mitochondria, a MTS which is longer than 30 aa and having at sufficient positively charge is required for the targeting.

The PBE is shown to be not essential for Yta10 targeting. So, it has to be further investigated whether the pre-localization of mRNA to mitochondria is not essential only for Yta10 or all the other proteins that utilize the same pathway as well.

The result showed that overall charge in MTS of Yta10 is critical and it seems to be involved in interaction with Tom70, given that Δ32-72 MTS variants showed poor growth in the Tom70 deletion strain. This result might be electrostatic interaction with Tom22 weakened [105-107].

Although the conventional *in vitro* mitochondrial protein import approach has successfully revealed the mechanism of mitochondrial protein targeting, it is time-consuming for isolation of mitochondria and incapable of monitoring the process in the cellular environment. We have come up with a growth complementation assay that allows rapid and simple assessment of protein targeting to mitochondria in vivo.

In summary, our results showed that 30 residues within the N-terminal 72 predicted presequence, 6 positively charged amino acids, and the 250bp of the 3'UTR are minimally required for efficient targeting of Yta10 to mitochondria.

3. 4. Material and Methods

Yeast strains

W303-1a (*MATa, ade2, can1, his3, leu2, trp1,* and *ura3*) was used as a parental strain in this study. *yta10*Δ (*MATa, ade2, can1, his3, leu2, trp1, ura3, yta10::HIS3MX6*) was made by standard homologous recombination, substituting *YTA10* with an amplified *HIS3MX6* [29]. The primers used for the amplification of HIS3MX6 cassette were 5' CAGCGTTTGCAGACGTTATCTCGGATCCCCGGGTTAATTAA 3' and 5' TTGGGTAGAACGGTGTATTGTGTTGAATTCGAGCTCGTTTAAAC 3'. yta10Δ was used to make *yta10*Δ*yta12*Δ (*MATa, ade2, can1, his3, leu2, trp1, ura3, yta10:: HIS3MX6, yta12::KanMX6*) by substituting *TOM70* with *KanMX6*. The primers used for the amplification of *KanMX6* cassette were 5' CGGAAGTGAAATTACAGCTCACATCTAGGTTCTCAATTGCCAATGcggatccc cgggttaattaa 3' and 5' CTTAGTTTTTGTCTTCTCCTAAAAGTTTTTAAGTTTATGTTTACTGTTTAgaa ttcgagctcgtttaaac 3'. These yeast strains were cultured at 30°C in this study.

Plasmid construction

YTA10 was amplified from the genomic DNA with using a set of primers; 5' ATAGGGCGAATTGGAGCTCCACCGCGGTGGCGTTGTACATATATCTGCT 3' and 5' TATCGATAAGCTTGATATCGAATTCCTGCAGGATTTAATAAATGAAGGTGT T 3'. Yta10 MTS variants were generated using [pRS314 *YTA10* WT] as template for site directed mutagenesis. *TOM70* was amplified from the genomic DNA with using a set of primers; 5' GGTGGCGGCCGCTCTAGAACTAGTGGATCCCTCAAAATTTTCATTGTCAA TGATAAAAGTC 3' and 5' ATCGATAAGCTTGATATCGAATTCCTGCACACCTCTTTGCTGTACCTTTAT G 3'.

Growth assay

*yta10*Δ expressing [pRS314 *YTA10* variants] were cultured in –Trp(Glucose) media overnight at 30°C. The overnight culture was diluted to 0.1 OD_{600} and cultured to 0.5

OD600 at 30°C. 10µl of culture was spotted on YPD or YPG (Glycerol) plate and further incubated for two days at 30°C. Photos were taken on Chemi-doc-XRS+ system using epi light (Bio-rad). *yta10*Δ/*tom70*Δ [pRS314 *YTA10* WT] expressing [pRS316 *TOM70*] were cultured in –Trp –Ura (Glucose) media overnight at 30°C. The overnight culture was diluted to 0.1 OD600 and cultured to 0.5 OD600 at 30°C. 10µl of culture was spotted on YPD or YPEG (Ethanol/Glycerol) plate and further incubated for two days at 30°C. Photos were taken on Chemi-doc-XRS+ system using epi light (Bio-rad).

Protein preparation and Western blotting

Preparation of lysates, SDS-PAGE and Western blotting were conducted as previously described [23]. Briefly, yeast transformants were grown overnight in 5 ml of SD media at 30 °C. Proteins were precipitated from 1 OD_{600} unit of yeast cells by addition of trichloroacetic acid (TCA, Sigma). Precipitated proteins were resuspended in 40µl of sample buffer and incubated for 5 min at 95°C prior to SDS-PAGE. The samples were separated on 6.5% or 12.5% Tris-HCl gels (Bio-rad) and followed by Western blotting. Membranes were immunodecorated with an anti-HA antibody (Covance) and developed with Amersham Bioscience Advanced ECL kit on a Chemi-doc-XRS+ system (Bio-rad). Quantification of detected bands was done using Image Lab 5.0 (Bio-rad).

Fluorescence microscopy

Yeast transformants expressing yEGFP fusion constructs were grown overnight in 5 ml of −Trp medium at 30 °C. 100µl of cells were taken from 0.6 $O.D._{600}$ culture. Cells were transferred to a 96 well plate for fluorescence assessment using a Zeiss Axiovert 200 M inverted microscope with a Plan-NeoFluar 100×/1.30 NA oil-immersion objective lens. Fluorescence images were taken using a standard fluoresceinisothiocyanate (FITC) filter set (excitation band pass filter, 450–490 nm; beam splitter, 510 nm; emission band pass filter, 515–565 nm). The pictures were taken with an exposure time of 0.2 ms [108] .

REFERENCE

1. Becker, T., et al., *Biogenesis of mitochondrial membrane proteins.* Curr Opin Cell Biol, 2009. **21**(4): p. 484-93.
2. Janska, H., M. Kwasniak, and J. Szczepanowska, *Protein quality control in organelles - AAA/FtsH story.* Biochim Biophys Acta, 2013. **1833**(2): p. 381-7.
3. Arlt, H., et al., *The YTA10-12 complex, an AAA protease with chaperone-like activity in the inner membrane of mitochondria.* Cell, 1996. **85**(6): p. 875-85.
4. Langklotz, S., U. Baumann, and F. Narberhaus, *Structure and function of the bacterial AAA protease FtsH.* Biochim Biophys Acta, 2012. **1823**(1): p. 40-8.
5. Tatsuta, T. and T. Langer, *AAA proteases in mitochondria: diverse functions of membrane-bound proteolytic machines.* Res Microbiol, 2009. **160**(9): p. 711-7.
6. Sauer, R.T. and T.A. Baker, *AAA+ proteases: ATP-fueled machines of protein destruction.* Annu Rev Biochem, 2011. **80**: p. 587-612.
7. Augustin, S., et al., *An intersubunit signaling network coordinates ATP hydrolysis by m-AAA proteases.* Mol Cell, 2009. **35**(5): p. 574-85.
8. Giaever, G. and C. Nislow, *The yeast deletion collection: a decade of functional genomics.* Genetics, 2014. **197**(2): p. 451-65.
9. Gerdes, F., T. Tatsuta, and T. Langer, *Mitochondrial AAA proteases--towards a molecular understanding of membrane-bound proteolytic machines.* Biochim Biophys Acta, 2012. **1823**(1): p. 49-55.
10. Ding, B., et al., *Dissecting Substrate Specificities of the Mitochondrial AFG3L2 Protease.* Biochemistry, 2018. **57**(28): p. 4225-4235.
11. Lee, S., et al., *Electron cryomicroscopy structure of a membrane-anchored mitochondrial AAA protease.* J Biol Chem, 2011. **286**(6): p. 4404-11.
12. Bonn, F., et al., *Presequence-dependent folding ensures MrpL32 processing by the m-AAA protease in mitochondria.* EMBO J, 2011.

30(13): p. 2545-56.

13. Tatsuta, T., et al., *m-AAA protease-driven membrane dislocation allows intramembrane cleavage by rhomboid in mitochondria.* EMBO J, 2007. **26**(2): p. 325-35.
14. Bauer, M., et al., *PET1402, a nuclear gene required for proteolytic processing of cytochrome oxidase subunit 2 in yeast.* Mol Gen Genet, 1994. **245**(3): p. 272-8.
15. Kihara, A., Y. Akiyama, and K. Ito, *Dislocation of membrane proteins in FtsH-mediated proteolysis.* EMBO J, 1999. **18**(11): p. 2970-81.
16. Leonhard, K., et al., *Membrane protein degradation by AAA proteases in mitochondria: extraction of substrates from either membrane surface.* Mol Cell, 2000. **5**(4): p. 629-38.
17. Nolden, M., et al., *The m-AAA protease defective in hereditary spastic paraplegia controls ribosome assembly in mitochondria.* Cell, 2005. **123**(2): p. 277-89.
18. Koppen, M. and T. Langer, *Protein degradation within mitochondria: versatile activities of AAA proteases and other peptidases.* Crit Rev Biochem Mol Biol, 2007. **42**(3): p. 221-42.
19. Arlt, H., et al., *The formation of respiratory chain complexes in mitochondria is under the proteolytic control of the m-AAA protease.* EMBO J, 1998. **17**(16): p. 4837-47.
20. Esser, K., et al., *A novel two-step mechanism for removal of a mitochondrial signal sequence involves the mAAA complex and the putative rhomboid protease Pcp1.* J Mol Biol, 2002. **323**(5): p. 835-43.
21. Botelho, S.C., et al., *Dislocation by the m-AAA protease increases the threshold hydrophobicity for retention of transmembrane helices in the inner membrane of yeast mitochondria.* J Biol Chem, 2013. **288**(7): p. 4792-8.
22. Lee, S., et al., *Molecular insights into the m-AAA protease-mediated dislocation of transmembrane helices in the mitochondrial inner membrane.* J Biol Chem, 2017. **292**(49): p. 20058-20066.
23. Park, K., et al., *Dissecting stop transfer versus conservative sorting pathways for mitochondrial inner membrane proteins in vivo.* J Biol

Chem, 2013. **288**(3): p. 1521-32.

24. Paetzel, M., et al., *Crystallographic and biophysical analysis of a bacterial signal peptidase in complex with a lipopeptide-based inhibitor.* J Biol Chem, 2004. **279**(29): p. 30781-90.
25. Arnold, I. and T. Langer, *Membrane protein degradation by AAA proteases in mitochondria.* Biochim Biophys Acta, 2002. **1592**(1): p. 89-96.
26. Graef, M., G. Seewald, and T. Langer, *Substrate recognition by AAA+ ATPases: distinct substrate binding modes in ATP-dependent protease Yme1 of the mitochondrial intermembrane space.* Mol Cell Biol, 2007. **27**(7): p. 2476-85.
27. Rampello, A.J. and S.E. Glynn, *Identification of a Degradation Signal Sequence within Substrates of the Mitochondrial i-AAA Protease.* J Mol Biol, 2017. **429**(6): p. 873-885.
28. Consolato, F., et al., *m-AAA and i-AAA complexes coordinate to regulate OMA1, the stress-activated supervisor of mitochondrial dynamics.* J Cell Sci, 2018. **131**(7).
29. Longtine, M.S., et al., *Additional modules for versatile and economical PCR-based gene deletion and modification in Saccharomyces cerevisiae.* Yeast, 1998. **14**(10): p. 953-61.
30. Bauer, M.F., et al., *Role of Tim23 as voltage sensor and presequence receptor in protein import into mitochondria.* Cell, 1996. **87**(1): p. 33-41.
31. Lohret, T.A., R.E. Jensen, and K.W. Kinnally, *Tim23, a protein import component of the mitochondrial inner membrane, is required for normal activity of the multiple conductance channel, MCC.* J Cell Biol, 1997. **137**(2): p. 377-86.
32. Genge, M.G. and D. Mokranjac, *Coordinated Translocation of Presequence-Containing Precursor Proteins Across Two Mitochondrial Membranes: Knowns and Unknowns of How TOM and TIM23 Complexes Cooperate With Each Other.* Front Physiol, 2021. **12**: p. 806426.
33. Gebert, M., et al., *Mgr2 promotes coupling of the mitochondrial presequence translocase to partner complexes.* J Cell Biol, 2012. **197**(5): p. 595-604.

34. Kaldi, K., et al., *Biogenesis of Tim23 and Tim17, integral components of the TIM machinery for matrix-targeted preproteins.* EMBO J, 1998. **17**(6): p. 1569-76.
35. Chacinska, A., et al., *Mitochondrial presequence translocase: switching between TOM tethering and motor recruitment involves Tim21 and Tim17.* Cell, 2005. **120**(6): p. 817-29.
36. Demishtein-Zohary, K., et al., *Role of Tim17 in coupling the import motor to the translocation channel of the mitochondrial presequence translocase.* Elife, 2017. **6**.
37. Matta, S.K., et al., *Role of Tim17 Transmembrane Regions in Regulating the Architecture of Presequence Translocase and Mitochondrial DNA Stability.* Mol Cell Biol, 2017. **37**(6).
38. Yamamoto, H., et al., *Tim50 is a subunit of the TIM23 complex that links protein translocation across the outer and inner mitochondrial membranes.* Cell, 2002. **111**(4): p. 519-28.
39. Guo, Y., et al., *Tim50, a component of the mitochondrial translocator, regulates mitochondrial integrity and cell death.* J Biol Chem, 2004. **279**(23): p. 24813-25.
40. Gevorkyan-Airapetov, L., et al., *Interaction of Tim23 with Tim50 Is essential for protein translocation by the mitochondrial TIM23 complex.* J Biol Chem, 2009. **284**(8): p. 4865-72.
41. Mokranjac, D., et al., *Role of Tim50 in the transfer of precursor proteins from the outer to the inner membrane of mitochondria.* Mol Biol Cell, 2009. **20**(5): p. 1400-7.
42. Schulz, C., et al., *Tim50's presequence receptor domain is essential for signal driven transport across the TIM23 complex.* J Cell Biol, 2011. **195**(4): p. 643-56.
43. Dayan, D., et al., *A mutagenesis analysis of Tim50, the major receptor of the TIM23 complex, identifies regions that affect its interaction with Tim23.* Sci Rep, 2019. **9**(1): p. 2012.
44. Chaudhuri, M., A. Tripathi, and F.S. Gonzalez, *Diverse Functions of Tim50, a Component of the Mitochondrial Inner Membrane Protein Translocase.* Int J Mol Sci, 2021. **22**(15).

45. Meier, S., W. Neupert, and J.M. Herrmann, *Conserved N-terminal negative charges in the Tim17 subunit of the TIM23 translocase play a critical role in the import of preproteins into mitochondria.* J Biol Chem, 2005. **280**(9): p. 7777-85.
46. Wiedemann, N., et al., *Sorting switch of mitochondrial presequence translocase involves coupling of motor module to respiratory chain.* J Cell Biol, 2007. **179**(6): p. 1115-22.
47. Chacinska, A., et al., *Distinct forms of mitochondrial TOM-TIM supercomplexes define signal-dependent states of preprotein sorting.* Mol Cell Biol, 2010. **30**(1): p. 307-18.
48. Merlin, A., et al., *The J-related segment of tim44 is essential for cell viability: a mutant Tim44 remains in the mitochondrial import site, but inefficiently recruits mtHsp70 and impairs protein translocation.* J Cell Biol, 1999. **145**(5): p. 961-72.
49. Hutu, D.P., et al., *Mitochondrial protein import motor: differential role of Tim44 in the recruitment of Pam17 and J-complex to the presequence translocase.* Mol Biol Cell, 2008. **19**(6): p. 2642-9.
50. Schiller, D., et al., *Residues of Tim44 involved in both association with the translocon of the inner mitochondrial membrane and regulation of mitochondrial Hsp70 tethering.* Mol Cell Biol, 2008. **28**(13): p. 4424-33.
51. Ting, S.Y., et al., *Dual interaction of scaffold protein Tim44 of mitochondrial import motor with channel-forming translocase subunit Tim23.* Elife, 2017. **6**.
52. van der Laan, M., et al., *Pam17 is required for architecture and translocation activity of the mitochondrial protein import motor.* Mol Cell Biol, 2005. **25**(17): p. 7449-58.
53. Mokranjac, D., et al., *The import motor of the yeast mitochondrial TIM23 preprotein translocase contains two different J proteins, Tim14 and Mdj2.* J Biol Chem, 2005. **280**(36): p. 31608-14.
54. Ting, S.Y., et al., *Architecture of the TIM23 inner mitochondrial translocon and interactions with the matrix import motor.* J Biol Chem, 2014. **289**(41): p. 28689-96.
55. Ieva, R., et al., *Mgr2 functions as lateral gatekeeper for preprotein*

sorting in the mitochondrial inner membrane. Mol Cell, 2014. **56**(5): p. 641-52.

56. Steffen, J. and C.M. Koehler, *The great escape: Mgr2 of the mitochondrial TIM23 translocon is a gatekeeper Tasked with releasing membrane proteins.* Mol Cell, 2014. **56**(5): p. 613-4.
57. Mirzalieva, O., et al., *Deletion of Mgr2p Affects the Gating Behavior of the TIM23 Complex.* Front Physiol, 2018. **9**: p. 1960.
58. Matta, S.K., A. Kumar, and P. D'Silva, *Mgr2 regulates mitochondrial preprotein import by associating with channel-forming Tim23 subunit.* Mol Biol Cell, 2020. **31**(11): p. 1112-1123.
59. Herrmann, J.M. and W. Neupert, *Protein insertion into the inner membrane of mitochondria.* IUBMB Life, 2003. **55**(4-5): p. 219-25.
60. Meier, S., W. Neupert, and J.M. Herrmann, *Proline residues of transmembrane domains determine the sorting of inner membrane proteins in mitochondria.* J Cell Biol, 2005. **170**(6): p. 881-8.
61. Gavel, Y. and G. von Heijne, *The distribution of charged amino acids in mitochondrial inner-membrane proteins suggests different modes of membrane integration for nuclearly and mitochondrially encoded proteins.* Eur J Biochem, 1992. **205**(3): p. 1207-15.
62. Bohnert, M., et al., *Cooperation of stop-transfer and conservative sorting mechanisms in mitochondrial protein transport.* Curr Biol, 2010. **20**(13): p. 1227-32.
63. Bykov, Y.S., et al., *Cytosolic Events in the Biogenesis of Mitochondrial Proteins.* Trends Biochem Sci, 2020. **45**(8): p. 650-667.
64. Matouschek, A., et al., *Active unfolding of precursor proteins during mitochondrial protein import.* EMBO J, 1997. **16**(22): p. 6727-36.
65. Lim, J.H., et al., *The mitochondrial Hsp70-dependent import system actively unfolds preproteins and shortens the lag phase of translocation.* EMBO J, 2001. **20**(5): p. 941-50.
66. Shiota, T., et al., *In vivo protein-interaction mapping of a mitochondrial translocator protein Tom22 at work.* Proc Natl Acad Sci U S A, 2011. **108**(37): p. 15179-83.
67. Young, J.C., N.J. Hoogenraad, and F.U. Hartl, *Molecular chaperones*

Hsp90 and Hsp70 deliver preproteins to the mitochondrial import receptor Tom70. Cell, 2003. **112**(1): p. 41-50.

68. Eliyahu, E., C. Lesnik, and Y. Arava, *The protein chaperone Ssa1 affects mRNA localization to the mitochondria.* FEBS Lett, 2012. **586**(1): p. 64-9.
69. Hasin, N., et al., *Global transcript and phenotypic analysis of yeast cells expressing Ssa1, Ssa2, Ssa3 or Ssa4 as sole source of cytosolic Hsp70-Ssa chaperone activity.* BMC Genomics, 2014. **15**(1): p. 194.
70. Opalinski, L., et al., *Recruitment of Cytosolic J-Proteins by TOM Receptors Promotes Mitochondrial Protein Biogenesis.* Cell Rep, 2018. **25**(8): p. 2036-2043 e5.
71. Jores, T., et al., *Cytosolic Hsp70 and Hsp40 chaperones enable the biogenesis of mitochondrial beta-barrel proteins.* J Cell Biol, 2018. **217**(9): p. 3091-3108.
72. Craig, E.A., *Hsp70 at the membrane: driving protein translocation.* BMC Biol, 2018. **16**(1): p. 11.
73. Gaur, D., et al., *Ydj1 interaction at nucleotide-binding-domain of yeast Ssa1 impacts Hsp90 collaboration and client maturation.* PLoS Genet, 2022. **18**(11): p. e1010442.
74. Hansen, K.G., A. Schlagowski, and J.M. Herrmann, *Escorted by chaperones: Sti1 helps to usher precursor proteins from the ribosome to mitochondria.* FEBS J, 2016. **283**(18): p. 3335-7.
75. Bhattacharya, K., et al., *The Hsp70-Hsp90 co-chaperone Hop/Stip1 shifts the proteostatic balance from folding towards degradation.* Nat Commun, 2020. **11**(1): p. 5975.
76. Williams, C.C., C.H. Jan, and J.S. Weissman, *Targeting and plasticity of mitochondrial proteins revealed by proximity-specific ribosome profiling.* Science, 2014. **346**(6210): p. 748-51.
77. Olivas, W. and R. Parker, *The Puf3 protein is a transcript-specific regulator of mRNA degradation in yeast.* EMBO J, 2000. **19**(23): p. 6602-11.
78. Wickens, M., et al., *A PUF family portrait: 3'UTR regulation as a way of life.* Trends Genet, 2002. **18**(3): p. 150-7.
79. Gerber, A.P., D. Herschlag, and P.O. Brown, *Extensive association of*

functionally and cytotopically related mRNAs with Puf family RNA-binding proteins in yeast. PLoS Biol, 2004. **2**(3): p. E79.

80. Garcia-Rodriguez, L.J., A.C. Gay, and L.A. Pon, *Puf3p, a Pumilio family RNA binding protein, localizes to mitochondria and regulates mitochondrial biogenesis and motility in budding yeast.* J Cell Biol, 2007. **176**(2): p. 197-207.
81. Saint-Georges, Y., et al., *Yeast mitochondrial biogenesis: a role for the PUF RNA-binding protein Puf3p in mRNA localization.* PLoS One, 2008. **3**(6): p. e2293.
82. Eliyahu, E., et al., *Tom20 mediates localization of mRNAs to mitochondria in a translation-dependent manner.* Mol Cell Biol, 2010. **30**(1): p. 284-94.
83. Gadir, N., et al., *Localization of mRNAs coding for mitochondrial proteins in the yeast Saccharomyces cerevisiae.* RNA, 2011. **17**(8): p. 1551-65.
84. Lesnik, C., et al., *Corrigendum: OM14 is a mitochondrial receptor for cytosolic ribosomes that supports co-translational import into mitochondria.* Nat Commun, 2015. **6**: p. 6813.
85. Lesnik, C., A. Golani-Armon, and Y. Arava, *Localized translation near the mitochondrial outer membrane: An update.* RNA Biol, 2015. **12**(8): p. 801-9.
86. Avendano-Monsalve, M.C., et al., *Positively charged amino acids at the N terminus of select mitochondrial proteins mediate early recognition by import proteins alphabeta'-NAC and Sam37.* J Biol Chem, 2022. **298**(6): p. 101984.
87. George, R., et al., *The nascent polypeptide-associated complex (NAC) promotes interaction of ribosomes with the mitochondrial surface in vivo.* FEBS Lett, 2002. **516**(1-3): p. 213-6.
88. Ott, A.K., et al., *Functional Dissection of the Nascent Polypeptide-Associated Complex in Saccharomyces cerevisiae.* PLoS One, 2015. **10**(11): p. e0143457.
89. Hegde, R.S. and E. Zavodszky, *Recognition and Degradation of Mislocalized Proteins in Health and Disease.* Cold Spring Harb Perspect Biol, 2019. **11**(11).

90. Hansen, K.G., et al., *An ER surface retrieval pathway safeguards the import of mitochondrial membrane proteins in yeast.* Science, 2018. **361**(6407): p. 1118-1122.
91. Papic, D., et al., *The role of Djp1 in import of the mitochondrial protein Mim1 demonstrates specificity between a cochaperone and its substrate protein.* Mol Cell Biol, 2013. **33**(20): p. 4083-94.
92. Brix, J., et al., *Distribution of binding sequences for the mitochondrial import receptors Tom20, Tom22, and Tom70 in a presequence-carrying preprotein and a non-cleavable preprotein.* J Biol Chem, 1999. **274**(23): p. 16522-30.
93. Backes, S., et al., *Tom70 enhances mitochondrial preprotein import efficiency by binding to internal targeting sequences.* J Cell Biol, 2018. **217**(4): p. 1369-1382.
94. Abe, Y., et al., *Structural basis of presequence recognition by the mitochondrial protein import receptor Tom20.* Cell, 2000. **100**(5): p. 551-60.
95. Yamamoto, H., et al., *Dual role of the receptor Tom20 in specificity and efficiency of protein import into mitochondria.* Proc Natl Acad Sci U S A, 2011. **108**(1): p. 91-6.
96. Doyle, S.R., et al., *Evidence of evolutionary constraints that influences the sequence composition and diversity of mitochondrial matrix targeting signals.* PLoS One, 2013. **8**(6): p. e67938.
97. Calvo, S.E., et al., *Comparative Analysis of Mitochondrial N-Termini from Mouse, Human, and Yeast.* Mol Cell Proteomics, 2017. **16**(4): p. 512-523.
98. Indio, V., et al., *The prediction of organelle-targeting peptides in eukaryotic proteins with Grammatical-Restrained Hidden Conditional Random Fields.* Bioinformatics, 2013. **29**(8): p. 981-8.
99. Savojardo, C., et al., *TPpred3 detects and discriminates mitochondrial and chloroplastic targeting peptides in eukaryotic proteins.* Bioinformatics, 2015. **31**(20): p. 3269-75.
100. Almagro Armenteros, J.J., et al., *Detecting sequence signals in targeting peptides using deep learning.* Life Sci Alliance, 2019. **2**(5).
101. Fukasawa, Y., et al., *MitoFates: improved prediction of mitochondrial*

targeting sequences and their cleavage sites. Mol Cell Proteomics, 2015. **14**(4): p. 1113-26.

102. Vogtle, F.N., et al., *Global analysis of the mitochondrial N-proteome identifies a processing peptidase critical for protein stability.* Cell, 2009. **139**(2): p. 428-39.

103. Cormack, B.P., et al., *Yeast-enhanced green fluorescent protein (yEGFP): a reporter of gene expression in Candida albicans.* Microbiology (Reading), 1997. **143 (Pt 2)**: p. 303-311.

104. Lapointe, C.P., et al., *Multi-omics Reveal Specific Targets of the RNA-Binding Protein Puf3p and Its Orchestration of Mitochondrial Biogenesis.* Cell Syst, 2018. **6**(1): p. 125-135 e6.

105. Nargang, F.E., et al., *Role of the negative charges in the cytosolic domain of TOM22 in the import of precursor proteins into mitochondria.* Mol Cell Biol, 1998. **18**(6): p. 3173-81.

106. Saeki, K., et al., *Identification of mammalian TOM22 as a subunit of the preprotein translocase of the mitochondrial outer membrane.* J Biol Chem, 2000. **275**(41): p. 31996-2002.

107. Su, J., et al., *Structural basis of Tom20 and Tom22 cytosolic domains as the human TOM complex receptors.* Proc Natl Acad Sci U S A, 2022. **119**(26): p. e2200158119.

108. Sung, M.K. and W.K. Huh, *In vivo quantification of protein-protein interactions in Saccharomyces cerevisiae using bimolecular fluorescence complementation assay.* J Microbiol Methods, 2010. **83**(2): p. 194-201.

국문초록

미토콘드리아 막 단백질의 표적화와 막 내 삽입 기작에 관한 연구

이서은

서울대학교 자연과학대학 생명과학부

대부분의 미토콘드리아 단백질은 세포핵 유전체에 암호화 되어 있으며, 호흡 사슬 복합체 생산, 미토콘드리아 단백질 항성성 유지, 미토콘드리아 결합 및 분리 역동성 등의 과정에 필수적인 기능을 합니다. 세포핵 유래 미토콘드리아 단백질의 생성 결함은 유기체에 악영향을 미칩니다. 따라서, 이 세포핵 유래 미토콘드리아 단백질의 생성 원리를 이해하는 것은 생명의 기본 원리를 이해하는데 뿐만 아니라, 미토콘드리아 관련 질병의 치료법 개발에 필수적입니다.

세포핵 유래 미토콘드리아 단백질의 합성 중 또는 후, 이 단백질들은 정확하게 미토콘드리아에 도착하고, 미토콘드리아 내부의 각 영역으로 이동해야 합니다. 미토콘드리아에 도달하기 위하여, 이 단백질들은 아미노 말단에 존재하는 미토콘드리아 표적 서열을 가지고 있습니다. 미토콘드리아 외부막에 도착한 후, 이 단백질들은 미토콘드리아 외막 수송체, TOM 복합체를 통해 외막을 가로질러 수송 됩니다. 이러한 단백질들 중, 미토콘드리아 내강이나 내막에 존재하는 단백질들은 미토콘드리아 내막 수송체, TIM23 복합체에 의해 분류 됩니다. 단백질 3차 구조 형성 또는 복합체 형성에 문제가 있는 단백질들은 미토콘드리아 단백질 항상성 유지를 위해 내막에 존재하는 *m*-AAA 복합체에 의해 분해 됩니다. 이 연구는 1) *m*-AAA에 의한 막 단백질 분류 기작 2) TIM23 복합체의 아단위 단백질, Mgr2가 막 단백질 삽입 효율에 미치는 영향 3) 미토콘드리아 단백질 표적화에 관한 자세한 이해를

목표로 합니다.

이 목표를 위하여, 첫째로 저는 *m*-AAA 복합체 의존적 내막 단백질의 내강 전위에 대한 *m*-AAA 복합체 막 고정 영역의 분자 기작을 알아보고자 하였습니다. 이를 위해, Mgm1 변이 단백질의 전위를 *m*-AAA 복합체의 막 고정 영역 결합 변이주에서 시험 하였습니다. 이를 통해, *m*-AAA 복합체의 아단위 단백질인 Yta10/12의 두번째 막 관통 영역이 내막 단백질의 전위에 중요함을 확인 하였습니다.

다음으로 TIM 복합체의 문지기 단백질로 알려진 Mgr2 단백질이 기질 막 단백질의 특성에 따라 기질 막 단백질의 막 삽입 효율에 미치는 영향을 분석하기 위하여, TIM 복합체의 기질 단백질로 알려진 Mgm1의 막 삽입 신호 서열 소수성 및 주변 전하 아미노산 변이체를 mgr2 상실 및 과발현 변이주에서 시험 하였습니다. 이를 통해, 중간 소수성 막 삽입 서열과 막삽입 서열 주변 양전하 아미노산이 Mgr2 의존적 막 삽입 조절에 중요함을 확인하였습니다.

마지막으로, 미토콘드리아 표적 서열에 존재하는 어떤 요소가 단백질의 미토콘드리아 표적 효율에 영향을 미치는지를 효모 세포 안에서 조사하고자 하였습니다. 이를 위하여, 길이, 소수성, 전하를 가진 아미노산 등의 변화를 가진 다양한 종류의 미토콘드리아 표적화 서열을 제작한 후, 이들의 단백질 표적화 효율을 효모 성장 실험, 세포 소단위 분리, 형광 현미경 등의 기법 등을 통해 측정 하였습니다. 이를 통해, 미토콘드리아 표적 서열의 길이와 전하를 띤 아미노산의 개수 등이 단백질 표적화 효율에 중요한 영향을 가지고 있음을 확인 하였습니다.

이 연구들을 통하여, 미토콘드리아 표적 서열에 의한 미토콘드리아 단백질 표적화와 Mgr2와 *m*-AAA 복합체 의존적 내막 단백질 분류의 분자적 원리에 대한 이해를 한층 향상 시킬 수 있었습니다.

주요 단어: 미토콘드리아 표적 서열, Mgr2, *m*-AAA 복합체, 미토콘드리아, 효모